

Received: 2023.12.16

Accepted: 2024.04.10

Available online: 2024.05.27

Published: 2024.06.02

ANXA5: A Key Regulator of Immune Cell Infiltration in Hepatocellular Carcinoma

Authors' Contribution:
Study Design A
Data Collection B
Statistical Analysis C
Data Interpretation D
Manuscript Preparation E
Literature Search F
Funds Collection G

A **Weichen Wang***
B **Dongquan Liu***
C **Jiaming Yao**
E **Zhongxu Yuan**
F **Liang Yan**
AG **Baoqiang Cao**

Department of Hepatobiliary Surgery, Anhui No. 2 Provincial People's Hospital, Hefei, Anhui, PR China

* Weichen Wang and Dongquan Liu contributed equally

Corresponding Author: Baoqiang Cao, e-mail: caobaoqiang@126.com

Financial support: This work was supported by the Youth Science Fund of Anhui Province (No. 2022xkj125)

Conflict of interest: None declared

Background: Hepatocellular carcinoma (HCC) poses a significant threat to human life and is the most prevalent form of liver cancer. The intricate interplay between apoptosis, a common form of programmed cell death, and its role in immune regulation stands as a crucial mechanism influencing tumor metastasis.

Material/Methods: Utilizing HCC samples from the TCGA database and 61 anoikis-related genes (ARGs) sourced from GeneCards, we analyzed the relationship between ARGs and immune cell infiltration in HCC. Subsequently, we identified long non-coding RNAs (lncRNAs) associated with ARGs, using the least absolute shrinkage and selection operator (LASSO) regression analysis to construct a robust prognostic model. The predictive capabilities of the model were then validated through examination in a single-cell dataset.

Results: Our constructed prognostic model, derived from lncRNAs linked to ARGs, comprised 11 significant lncRNAs: NRAV, MCM3AP-AS1, OTUD6B-AS1, AC026356.1, AC009133.1, DDX11-AS1, AC108463.2, MIR4435-2HG, WARS2-AS1, LINC01094, and HCG18. The risk score assigned to HCC samples demonstrated associations with immune indicators and the infiltration of immune cells. Further, we identified Annexin A5 (ANXA5) as the pivotal gene among ARGs, with it exerting a prominent role in regulating the lncRNA gene signature. Our validation in a single-cell database elucidated the involvement of ANXA5 in immune cell infiltration, specifically in the regulation of mononuclear cells.

Conclusions: This study delves into the intricate correlation between ARGs and immune cell infiltration in HCC, culminating in the development of a novel prognostic model reliant on 11 ARGs-associated lncRNAs. Furthermore, our findings highlight ANXA5 as a promising target for immune regulation in HCC, offering new perspectives for immune therapy in the context of HCC.

Keywords: **Biomarkers, Tumor • Tumor Microenvironment • Biomarkers**

Full-text PDF: <https://www.medscimonit.com/abstract/index/idArt/943523>



Publisher's note: All claims expressed in this article are solely those of the authors and do not necessarily represent those of their affiliated organizations, or those of the publisher, the editors and the reviewers. Any product that may be evaluated in this article, or claim that may be made by its manufacturer, is not guaranteed or endorsed by the publisher

Introduction

Hepatocellular carcinoma (HCC) is the most prevalent form of liver cancer and is responsible for the fourth highest number of cancer-related deaths worldwide. Risk factors include chronic hepatitis B and C, alcohol addiction, metabolic liver disease, especially non-alcoholic fatty liver disease, and dietary toxins, such as aflatoxin [1].

Various reprogramming in HCC is one of the important causes of tumor progression [2]. Recent advances in anti-cancer immunotherapy, including inhibition of programmed cell death protein-1 (PD-1)/PD-L1, cytotoxic T-lymphocyte-associated protein-4 (CTLA4), various immune cell therapies, and vaccines, have improved the survival rates of patients with HCC to some extent [3]. The effectiveness of immunotherapy is related to the infiltration of various immune cells in the tumor microenvironment (TME) of HCC [4]. However, the complex regulation of immune cells and various factors in the TME lead to the tumor heterogeneity of HCC, highlighting the need for a deeper understanding of its molecular mechanisms for personalized patient treatment [5].

Immune suppressive cells, such as myeloid-derived suppressor cells, tumor-associated macrophages (TAMs), tumor-associated neutrophils, cancer-associated fibroblasts, and Tregs, are critical components of the TME that promote the growth and invasion of HCC [6]. HBV-specific CD8 T cells, HBV non-specific CD8 cells, CD4 T cells, B cells, natural killer cells, natural killer T cells, Kupffer cells, and hepatic stellate cells all participate in HBV-related HCC occurrence [7]. CCL18+ TAMs are associated with poor prognosis in HCC, as they impair the function of cytotoxic T cells [8]. Fetal-like TAMs can promote HCC progression by interacting with PLVAP+ endothelial cells [9]. Cancer-associated fibroblasts in HCC induce immune suppression phenotypes by secreting cytokines and recruiting monocytes and dendritic cells, thereby promoting immune evasion, tumor growth, and metastasis [10,11]. The infiltration of fibroblasts and macrophages in the TME is associated with immune therapy responses [12]. However, the intricate regulation of immune cells and various factors in the TME contribute to the tumor heterogeneity of HCC, underscoring the necessity for a deeper comprehension of its molecular mechanisms to tailor personalized patient treatments [5].

Anoikis, a common type of programmed cell death, is primarily associated with the interaction between the extracellular matrix and cells [13]. In tumors, anoikis is often disrupted and is a crucial mechanism for tumor metastasis [14]. The abnormal infiltration of immune cells in tumors is closely related to anoikis, and together they regulate tumor metastasis [14]. During tumor progression, detached tumor cells bypass the death signaling pathway and evade immune recognition,

which is the primary reason for the development of anoikis resistance [15]. However, a systematic analysis of the interaction between anoikis-related genes (ARGs) and tumor immune cells is still lacking in HCC.

Long non-coding RNAs (lncRNAs) are RNA molecules longer than 200 nt that do not have protein-coding functions [16]. They play a crucial role in homeostasis and tumorigenesis [17] and serve as tumor markers for early screening, diagnosis, prognosis, and predicting responses to medication [18,19]. lncRNA-related models are essential in colon cancer [19], lung adenocarcinoma [20], pancreatic adenocarcinoma [21], and other cancers. lncRNAs regulate the expression, localization, stability, and activity of their binding partners, triggering a series of carcinogenic phenotypes, such as sustained proliferation, metabolic abnormalities, increased stemness, and metastasis, leading to the occurrence and progression of HCC [22]. A novel lncRNA, RP11-386G11.10, reprograms lipid metabolism to promote the progression of HCC [23]. lncRNA HEPFAL accelerates ferroptosis in HCC by regulating the ubiquitination of SLC7A11 [24]. In the study of Liu et al, LINC01234 promoted HCC progression by coordinating aspartate metabolism reprogramming, which means that lncRNAs have an important role in HCC [25].

Therefore, this study focused on analyzing HCC samples from The Cancer Genome Atlas (TCGA) database to investigate the relationship between ARGs and the mutual regulation of immune cells. We developed a novel risk model based on 11 ARG-related lncRNAs and identified new regulatory targets for HCC immune cells. Furthermore, we validated our findings using HCC single-cell sequencing data from the Gene Expression Omnibus (GEO) database. In single-cell data, we observed a close association between the key gene Annexin A5 (ANXA5) and immune cells in ARGs. These findings hold significant implications for studying the TME of HCC and exploring immune-related therapeutic targets, providing theoretical support for subsequent clinical translation. This study provides new molecular targets for the immunotherapy of HCC and new research avenues for the regulation of anoikis and immune cells.

Material and Methods

Data Collection

We obtained transcriptome sequencing data and clinical information of HCC from the TCGA database (<https://portal.gdc.cancer.gov/>) [26], comprising 50 samples of normal liver tissue and 374 samples of HCC. The corresponding clinical characteristics of patients are presented in **Table 1**. Additionally, we retrieved single-cell sequencing data (GSE125449) of HCC from the GEO database (<https://www.ncbi.nlm.nih.gov/geo/>) [27].

Table 1. The clinical characteristics of patients with hepatocellular carcinoma.

Id	Age	Gender	Grade	Stage	T	M	N
TCGA-KR-A7K0	65	MALE	G1	Stage I	T1	M0	NO
TCGA-DD-A4NS	61	FEMALE	G2	Stage I	T1	M0	NO
TCGA-DD-AAED	51	MALE	G3	Stage I	T1	M0	NO
TCGA-DD-AADB	51	MALE	G4	Stage I	T1	M0	NO
TCGA-G3-A25V	68	MALE	G2	Stage I	T1	M0	NO
TCGA-DD-AAE7	72	MALE	G2	Stage I	T1	M0	NO
TCGA-LG-A9QC	48	MALE	G2	Stage I	T1	M0	NX
TCGA-DD-AAEH	73	MALE	G2	Stage I	T1	M0	NO
TCGA-2Y-A9H9	70	MALE	G2	Stage I	T1	MX	NO
TCGA-DD-A73B	72	FEMALE	G2	Stage I	T1	M0	NO
TCGA-UB-A7MD	67	MALE	G3	Stage I	T1	MX	NO
TCGA-5C-A9VH	70	MALE	G2	Stage I	T1	M0	NO
TCGA-ED-A627	74	MALE	G2	Stage I	T1	M0	NX
TCGA-G3-AAV2	50	MALE	G1	Stage I	T1	M0	NO
TCGA-GJ-A9DB	68	MALE	G2	Stage I	T1	MX	NO
TCGA-G3-AAV4	83	FEMALE	G1	Stage I	T1	M0	NO
TCGA-DD-AADP	45	MALE	G3	Stage I	T1	M0	NO
TCGA-DD-A4NL	46	MALE	G1	Stage I	T1	M0	NO
TCGA-2Y-A9GW	64	MALE	G2	Stage I	T1	MX	NO
TCGA-UB-A7ME	51	MALE	G2	Stage I	T1	MX	NX
TCGA-XR-A8TF	74	MALE	G1	Stage I	T1	MX	NX
TCGA-K7-A6G5	66	MALE	G2	Stage I	T1	MX	NO
TCGA-DD-A39Y	67	MALE	G3	Stage I	T1	M0	NX
TCGA-DD-A1E9	70	MALE	G2	Stage I	T1	M0	NO
TCGA-DD-A1EC	20	FEMALE	G3	Stage I	T1	M0	NO
TCGA-HP-A5MZ	78	MALE	G2	Stage I	T1	M0	NX
TCGA-DD-AAE2	51	MALE	G3	Stage I	T1	M0	NO
TCGA-NI-A8LF	74	MALE	G3	Stage I	T1	MX	NX
TCGA-DD-A1EF	57	FEMALE	G3	Stage I	T1	M0	NO
TCGA-GJ-A3OU	59	MALE	G2	Stage I	T1	MX	NX
TCGA-DD-AAD3	43	MALE	G2	Stage I	T1	M0	NO
TCGA-2Y-A9GU	55	FEMALE	G2	Stage I	T1	MX	NX
TCGA-DD-AACA	65	MALE	G3	Stage I	T1	M0	NO
TCGA-DD-AAW2	69	MALE	G2	Stage I	T1	M0	NO
TCGA-DD-AADD	51	MALE	G4	Stage I	T1	M0	NO

Table 1 continued. The clinical characteristics of patients with hepatocellular carcinoma.

Id	Age	Gender	Grade	Stage	T	M	N
TCGA-XR-A8TG	58	MALE	G2	Stage I	T1	M0	NX
TCGA-BC-A69I	69	MALE	G1	Stage I	T1	M0	N0
TCGA-DD-AAE3	50	MALE	G2	Stage I	T1	M0	N0
TCGA-EP-A3JL	76	MALE	G2	Stage I	T1	MX	NX
TCGA-G3-A25Z	58	MALE	G2	Stage I	T1	M0	N0
TCGA-DD-AAE6	59	FEMALE	G2	Stage I	T1	M0	N0
TCGA-EP-A2KC	62	MALE	G3	Stage I	T1	MX	NX
TCGA-DD-AADN	59	MALE	G4	Stage I	T1	MX	NX
TCGA-DD-AADR	58	MALE	G3	Stage I	T1	M0	N0
TCGA-G3-A3CG	80	MALE	G2	Stage I	T1	M0	N0
TCGA-DD-AACB	74	FEMALE	G3	Stage I	T1	M0	N0
TCGA-DD-AAEE	55	MALE	G4	Stage I	T1	M0	N0
TCGA-RC-A7SK	59	MALE	G3	Stage I	T1	M0	N0
TCGA-DD-AACL	66	FEMALE	G3	Stage I	T1	M0	N0
TCGA-DD-AAEC	62	MALE	G3	Stage I	T1	M0	N0
TCGA-DD-A4NR	85	FEMALE	G3	Stage I	T1	M0	N0
TCGA-BC-A10Z	62	FEMALE	G2	Stage I	T1	MX	N0
TCGA-DD-AACK	70	MALE	G2	Stage I	T1	M0	N0
TCGA-DD-AAW3	69	MALE	G2	Stage I	T1	M0	N0
TCGA-DD-A73F	77	FEMALE	G1	Stage I	T1	M0	N0
TCGA-DD-AACS	39	MALE	G3	Stage I	T1	M0	N0
TCGA-2Y-A9H2	64	FEMALE	G3	Stage I	T1	MX	N0
TCGA-DD-AAEG	59	FEMALE	G3	Stage I	T1	M0	N0
TCGA-DD-AACO	40	MALE	G3	Stage I	T1	M0	N0
TCGA-DD-AAVS	56	MALE	G2	Stage I	T1	M0	N0
TCGA-XR-A8TC	43	FEMALE	G2	Stage I	T1	MX	NX
TCGA-DD-AAVZ	38	MALE	G2	Stage I	T1	M0	N0
TCGA-EP-A2KB	46	FEMALE	G2	Stage I	T1	MX	NX
TCGA-G3-AAUZ	48	MALE	G2	Stage I	T1	M0	N0
TCGA-DD-A11D	57	FEMALE	G2	Stage I	T1	M0	N0
TCGA-DD-AACF	68	MALE	G3	Stage I	T1	M0	N0
TCGA-BD-A3EP	75	FEMALE	G2	Stage I	T1	M0	N0
TCGA-DD-A11A	67	MALE	G3	Stage I	T1	M0	N0
TCGA-DD-AADL	58	MALE	G4	Stage I	T1	M0	N0
TCGA-2Y-A9H6	68	FEMALE	G2	Stage I	T1	MX	NX

Table 1 continued. The clinical characteristics of patients with hepatocellular carcinoma.

Id	Age	Gender	Grade	Stage	T	M	N
TCGA-DD-A73E	66	MALE	G1	Stage I	T1	M0	N0
TCGA-RC-A7SF	66	MALE	G2	Stage I	T1	M0	N0
TCGA-DD-AAVP	48	MALE	G1	Stage I	T1	M0	N0
TCGA-DD-AACW	43	MALE	G3	Stage I	T1	M0	N0
TCGA-G3-A7M5	76	MALE	G2	Stage I	T1	MX	NX
TCGA-DD-AADY	55	FEMALE	G2	Stage I	T1	M0	N0
TCGA-DD-AACY	61	MALE	G3	Stage I	T1	M0	N0
TCGA-DD-A1EI	46	MALE	G2	Stage I	T1	M0	N0
TCGA-2Y-A9HB	66	MALE	G2	Stage I	T1	MX	NX
TCGA-ES-A2HS	80	MALE	G2	Stage I	T1	MX	NX
TCGA-FV-A2QQ	80	MALE	G2	Stage I	T1	MX	N0
TCGA-DD-AACU	59	MALE	G3	Stage I	T1	M0	N0
TCGA-DD-AACT	69	FEMALE	G2	Stage I	T1	M0	N0
TCGA-FV-A2QR	75	MALE	G1	Stage I	T1	M0	N0
TCGA-DD-A1EB	72	FEMALE	G2	Stage I	T1	M0	N0
TCGA-DD-AAVQ	38	MALE	G2	Stage I	T1	M0	N0
TCGA-G3-A25U	63	FEMALE	G3	Stage I	T1	M0	N0
TCGA-G3-A7M8	31	MALE	G1	Stage I	T1	MX	NX
TCGA-DD-AACZ	63	FEMALE	G4	Stage I	T1	M0	N0
TCGA-MI-A75C	64	MALE	G3	Stage I	T1	M0	N0
TCGA-DD-A4NP	32	MALE	G3	Stage I	T1	M0	N0
TCGA-DD-AADF	64	FEMALE	G4	Stage I	T1	M0	N0
TCGA-DD-AAEA	65	MALE	G3	Stage I	T1	M0	N0
TCGA-G3-A5SJ	59	MALE	G2	Stage I	T1	M0	NX
TCGA-DD-AAD0	73	FEMALE	G2	Stage I	T1	M0	N0
TCGA-DD-AAEI	72	MALE	G2	Stage I	T1	M0	N0
TCGA-2Y-A9GT	51	MALE	G2	Stage I	T1	MX	NX
TCGA-2Y-A9H4	68	MALE	G2	Stage I	T1	MX	N0
TCGA-DD-AACD	48	MALE	G4	Stage I	T1	M0	N0
TCGA-2Y-A9GV	54	FEMALE	G1	Stage I	T1	MX	NX
TCGA-DD-AADJ	70	FEMALE	G3	Stage I	T1	M0	N0
TCGA-G3-AAV0	58	MALE	G2	Stage I	T1	M0	N0
TCGA-DD-AAC8	72	MALE	G3	Stage I	T1	M0	N0
TCGA-WJ-A86L	68	FEMALE	G2	Stage I	T1	MX	NX
TCGA-G3-A7M7	65	MALE	G1	Stage I	T1	MX	NX

Table 1 continued. The clinical characteristics of patients with hepatocellular carcinoma.

Id	Age	Gender	Grade	Stage	T	M	N
TCGA-DD-AADC	53	MALE	G3	Stage I	T1	M0	N0
TCGA-DD-AACC	61	MALE	G2	Stage I	T1	M0	N0
TCGA-WX-AA44	64	FEMALE	G3	Stage I	T1	MX	NX
TCGA-DD-AAD5	54	MALE	G3	Stage I	T1	M0	N0
TCGA-2Y-A9H7	81	FEMALE	G2	Stage I	T1	MX	N0
TCGA-DD-A4NO	65	MALE	G1	Stage I	T1	M0	N0
TCGA-G3-A25Y	52	FEMALE	G3	Stage I	T1	M0	N0
TCGA-BC-A3KF	66	FEMALE	G2	Stage I	T1	M0	NX
TCGA-DD-AAVR	44	MALE	G2	Stage I	T1	M0	N0
TCGA-ES-A2HT	54	MALE	G2	Stage I	T1	MX	NX
TCGA-DD-AADI	43	FEMALE	G3	Stage I	T1	M0	N0
TCGA-DD-AADW	48	MALE	G3	Stage I	T1	M0	N0
TCGA-FV-A4ZQ	52	MALE	G2	Stage I	T1	M0	NX
TCGA-DD-AAW0	54	MALE	G2	Stage I	T1	M0	N0
TCGA-DD-A73G	73	FEMALE	G3	Stage I	T1	M0	N0
TCGA-DD-A11B	73	MALE	G2	Stage I	T1	M0	N0
TCGA-DD-AADS	63	MALE	G2	Stage I	T1	M0	N0
TCGA-MR-A520	58	MALE	G1	Stage I	T1	MX	NX
TCGA-FV-A496	84	FEMALE	G2	Stage I	T1	M0	NX
TCGA-DD-AA3A	81	FEMALE	G4	Stage I	T1	MX	N0
TCGA-DD-A73A	71	MALE	G2	Stage I	T1	M0	N0
TCGA-BW-A5NQ	63	MALE	G3	Stage I	T1	MX	NX
TCGA-DD-A4NB	25	MALE	G2	Stage I	T1	M0	N0
TCGA-DD-AADO	55	MALE	G3	Stage I	T1	M0	N0
TCGA-FV-A3R3	38	FEMALE	G2	Stage I	T1	MX	NX
TCGA-DD-AAD2	66	MALE	G2	Stage I	T1	M0	N0
TCGA-DD-A1EG	76	MALE	G3	Stage I	T1	M0	N0
TCGA-G3-A3CI	71	MALE	G2	Stage I	T1	M0	N0
TCGA-DD-AAD1	51	FEMALE	G4	Stage I	T1	M0	N0
TCGA-DD-A11C	69	MALE	G3	Stage I	T1	M0	N0
TCGA-2Y-A9H5	59	FEMALE	G3	Stage I	T1	MX	N0
TCGA-EP-A12J	62	MALE	G1	Stage I	T1	MX	NX
TCGA-DD-AACP	64	MALE	G3	Stage I	T1	M0	N0
TCGA-DD-A3A2	76	FEMALE	G1	Stage I	T1	M0	N0
TCGA-DD-A3A0	70	MALE	G2	Stage I	T1	M0	NX

Table 1 continued. The clinical characteristics of patients with hepatocellular carcinoma.

Id	Age	Gender	Grade	Stage	T	M	N
TCGA-DD-A4ND	56	FEMALE	G3	Stage I	T1	M0	NO
TCGA-DD-AAEB	60	MALE	G2	Stage I	T1	M0	NO
TCGA-G3-A25S	64	MALE	G2	Stage I	T1	M0	NO
TCGA-DD-AAE4	49	FEMALE	G1	Stage I	T1	M0	NO
TCGA-DD-AAD8	73	FEMALE	G2	Stage I	T1	M0	NO
TCGA-DD-AAE9	69	MALE	G3	Stage I	T1	M0	NO
TCGA-DD-AADA	66	FEMALE	G3	Stage I	T1	M0	NO
TCGA-DD-A39X	78	FEMALE	G2	Stage I	T1	M0	NX
TCGA-DD-AADE	50	MALE	G4	Stage I	T1	M0	NO
TCGA-K7-A5RG	66	MALE	G1	Stage I	T1	MX	NX
TCGA-DD-AAVW	35	MALE	G2	Stage I	T1	M0	NO
TCGA-MR-A8JO	34	MALE	G3	Stage I	T1	MX	NO
TCGA-DD-AAE1	52	MALE	G3	Stage I	T1	M0	NO
TCGA-DD-A4NN	56	FEMALE	G3	Stage I	T1	M0	NO
TCGA-G3-A3CK	61	MALE	G2	Stage I	T1	M0	NO
TCGA-EP-A26S	70	MALE	G2	Stage I	T1	MX	NO
TCGA-2Y-A9GX	68	MALE	G2	Stage I	T1	MX	NX
TCGA-RC-A7S9	47	FEMALE	G3	Stage I	T1	M0	NO
TCGA-DD-A3A3	45	MALE	G2	Stage I	T1	M0	NO
TCGA-O8-A75V	54	MALE	G2	Stage I	T1	MX	NX
TCGA-K7-A5RF	64	MALE	G1	Stage I	T1	MX	NX
TCGA-G3-A5SK	58	MALE	G1	Stage I	T1	M0	NX
TCGA-DD-A1ED	68	MALE	G1	Stage I	T1	M0	NO
TCGA-DD-AACV	53	MALE	G3	Stage I	T1	M0	NO
TCGA-2Y-A9H1	58	MALE	G2	Stage I	T1	MX	NX
TCGA-DD-A4NF	72	MALE	G2	Stage I	T1	M0	NO
TCGA-KR-A7K2	64	MALE	G1	Stage I	T1	M0	NO
TCGA-DD-AAC9	51	MALE	G2	Stage I	T1	M0	NO
TCGA-DD-AACN	32	MALE	G3	Stage I	T1	M0	NO
TCGA-DD-AAE8	45	MALE	G3	Stage I	T1	M0	NO
TCGA-DD-AADV	50	MALE	G3	Stage I	T1	M0	NO
TCGA-G3-A7M6	60	FEMALE	G3	Stage I	T1	MX	NX
TCGA-KR-A7K8	57	MALE	G1	Stage I	T1	M0	NO
TCGA-DD-A1EA	68	MALE	G2	Stage II	T2	M0	NO
TCGA-G3-AAV7	38	MALE	G2	Stage II	T2	M0	NO

Table 1 continued. The clinical characteristics of patients with hepatocellular carcinoma.

Id	Age	Gender	Grade	Stage	T	M	N
TCGA-5C-AAPD	61	MALE	G1	Stage II	T2	M0	N0
TCGA-DD-A113	55	FEMALE	G3	Stage II	T2	M0	N0
TCGA-ED-A5KG	60	FEMALE	G2	Stage II	T2	M0	N0
TCGA-DD-A39V	77	MALE	G3	Stage II	T2	M0	NX
TCGA-ZS-A9CD	73	MALE	G2	Stage II	T2	MX	NX
TCGA-CC-5261	44	MALE	G2	Stage II	T2	M0	N0
TCGA-4R-AA8I	66	MALE	G2	Stage II	T2	MX	NX
TCGA-DD-AADQ	59	MALE	G3	Stage II	T2	M0	N0
TCGA-DD-AAVU	46	MALE	G2	Stage II	T2	M0	N0
TCGA-MI-A75G	63	MALE	G2	Stage II	T2	M0	N0
TCGA-G3-A25X	73	MALE	G3	Stage II	T2	M0	N0
TCGA-DD-AACX	66	MALE	G3	Stage II	T2	M0	N0
TCGA-UB-AA0U	60	MALE	G2	Stage II	T2	MX	NX
TCGA-RG-A7D4	69	MALE	G2	Stage II	T2	M0	N0
TCGA-DD-AAVX	38	MALE	G2	Stage II	T2	M0	N0
TCGA-CC-A7IJ	56	MALE	G3	Stage II	T2	M0	N0
TCGA-RC-A6M3	24	MALE	G3	Stage II	T2	M0	N0
TCGA-DD-A1EL	23	MALE	G3	Stage II	T2	M0	N0
TCGA-CC-5258	48	MALE	G2	Stage II	T2	M0	N0
TCGA-ED-A7PY	20	FEMALE	G3	Stage II	T2	M0	NX
TCGA-DD-AADU	60	MALE	G3	Stage II	T2	M0	N0
TCGA-DD-AAEK	51	MALE	G3	Stage II	T2	M0	N0
TCGA-2Y-A9GZ	82	FEMALE	G2	Stage II	T2	MX	NX
TCGA-G3-A3CJ	52	MALE	G2	Stage II	T2	M0	N0
TCGA-ED-A7PZ	61	MALE	G2	Stage II	T2	M0	NX
TCGA-DD-AACI	69	MALE	G3	Stage II	T2	M0	N0
TCGA-ZS-A9CF	64	MALE	G2	Stage II	T2	MX	NX
TCGA-RC-A6M6	75	MALE	G3	Stage II	T2	M0	NX
TCGA-5R-AA1C	57	MALE	G2	Stage II	T2	M0	N0
TCGA-ZS-A9CE	79	FEMALE	G1	Stage II	T2	MX	NX
TCGA-BC-A69H	64	MALE	G3	Stage II	T2	M0	NX
TCGA-G3-A5SL	70	MALE	G2	Stage II	T2	M0	NX
TCGA-ED-A7XP	53	FEMALE	G3	Stage II	T2	M0	N0
TCGA-DD-A4NI	67	MALE	G2	Stage II	T2	M0	NX
TCGA-WQ-AB4B	62	MALE	G2	Stage II	T2	M0	NX

Table 1 continued. The clinical characteristics of patients with hepatocellular carcinoma.

Id	Age	Gender	Grade	Stage	T	M	N
TCGA-DD-AACM	48	MALE	G3	Stage II	T2	M0	N0
TCGA-ED-A4XI	58	MALE	G3	Stage II	T2	M0	N0
TCGA-QA-A7B7	48	MALE	G2	Stage II	T2	MX	NX
TCGA-2Y-A9GY	64	FEMALE	G3	Stage II	T2	MX	NX
TCGA-BC-A3KG	68	FEMALE	G3	Stage II	T2	M0	N0
TCGA-ED-A459	47	MALE	G2	Stage II	T2	M0	N0
TCGA-BD-A3ER	62	MALE	G2	Stage II	T2	MX	NX
TCGA-G3-A5SM	58	MALE	G3	Stage II	T2	M0	NX
TCGA-RC-A7SH	42	MALE	G3	Stage II	T2	M0	N0
TCGA-DD-A73D	68	FEMALE	G1	Stage II	T2	MX	NX
TCGA-DD-AADK	68	FEMALE	G3	Stage II	T2	M0	N0
TCGA-CC-A7IG	47	MALE	G2	Stage II	T2	M0	N0
TCGA-DD-A118	77	FEMALE	G2	Stage II	T2	M0	N0
TCGA-5R-AAAM	65	FEMALE	G2	Stage II	T2	M0	N0
TCGA-BC-A217	75	FEMALE	G3	Stage II	T2	M0	NX
TCGA-FV-A495	51	FEMALE	G2	Stage II	T2	M0	NX
TCGA-FV-A3I0	76	FEMALE	G2	Stage II	T2	M0	NX
TCGA-UB-A7MB	24	MALE	G3	Stage II	T2	MX	NX
TCGA-LG-A6GG	79	FEMALE	G2	Stage II	T2	M0	NX
TCGA-DD-AACQ	50	MALE	G3	Stage II	T2	M0	N0
TCGA-KR-A7K7	61	FEMALE	G1	Stage II	T2	M0	N0
TCGA-DD-A4NJ	54	FEMALE	G2	Stage II	T2	M0	N0
TCGA-DD-AAVV	56	MALE	G3	Stage II	T2	M0	N0
TCGA-2Y-A9HA	70	MALE	G2	Stage II	T2	MX	NX
TCGA-DD-A39Z	43	FEMALE	G2	Stage II	T2	M0	NX
TCGA-CC-A9FS	55	MALE	G2	Stage II	T2	M0	N0
TCGA-UB-A7MA	62	FEMALE	G2	Stage II	T2b	M0	N0
TCGA-ZS-A9CG	55	MALE	G2	Stage II	T2	MX	NX
TCGA-DD-AADM	58	MALE	G3	Stage II	T2	M0	N0
TCGA-K7-AAU7	61	MALE	G2	Stage II	T2a	MX	NX
TCGA-WX-AA46	61	MALE	G1	Stage II	T2	MX	NX
TCGA-5C-A9VG	58	MALE	G2	Stage II	T2	M0	N0
TCGA-RC-A7SB	53	MALE	G2	Stage II	T2	M0	N0
TCGA-2Y-A9H3	45	MALE	G1	Stage II	T2	MX	NX
TCGA-G3-AAV5	67	MALE	G2	Stage II	T2	M0	N0

Table 1 continued. The clinical characteristics of patients with hepatocellular carcinoma.

Id	Age	Gender	Grade	Stage	T	M	N
TCGA-DD-AACH	69	MALE	G3	Stage II	T2	M0	N0
TCGA-G3-A5SI	44	MALE	G2	Stage II	T2	M0	N0
TCGA-CC-A8HV	51	FEMALE	G2	Stage II	T2	M0	N0
TCGA-DD-A3A6	72	FEMALE	G2	Stage II	T2	M0	N0
TCGA-DD-A4NQ	60	MALE	G3	Stage II	T2	M0	N0
TCGA-G3-AAV3	58	FEMALE	G2	Stage II	T2	M0	N0
TCGA-DD-AACG	52	MALE	G4	Stage II	T2	M0	N0
TCGA-DD-AACJ	75	MALE	G2	Stage II	T2	M0	N0
TCGA-GJ-A6C0	75	FEMALE	G2	Stage II	T2	MX	NX
TCGA-FV-A3I1	81	FEMALE	G2	Stage II	T2	MX	N0
TCGA-ED-A7PX	48	FEMALE	G3	Stage II	T2	M0	NX
TCGA-DD-A3A8	75	MALE	G2	Stage II	T2	M0	N0
TCGA-DD-A39W	29	FEMALE	G2	Stage III	T3	M0	N0
TCGA-DD-A3A5	66	FEMALE	G2	Stage III	T3	M0	N0
TCGA-DD-A1EH	23	MALE	G3	Stage III	T3	M0	N0
TCGA-CC-A5UC	63	MALE	G3	Stage IIIA	T3	M0	N0
TCGA-DD-AAE0	45	FEMALE	G4	Stage IIIA	T3a	M0	N0
TCGA-CC-A3M9	45	MALE	G3	Stage IIIA	T3	M0	N0
TCGA-DD-A3A4	37	MALE	G3	Stage IIIA	T3	M0	N0
TCGA-DD-AAW1	55	MALE	G2	Stage IIIA	T3	M0	N0
TCGA-EP-A2KA	52	FEMALE	G3	Stage IIIA	T3a	MX	NX
TCGA-UB-A7MC	59	MALE	G3	Stage IIIA	T3a	MX	N0
TCGA-CC-A7IF	59	MALE	G1	Stage IIIA	T3	M0	N0
TCGA-DD-A73C	65	FEMALE	G1	Stage IIIA	T3a	M0	N0
TCGA-ED-A97K	54	MALE	G2	Stage IIIA	T3a	M0	N0
TCGA-CC-A7II	54	MALE	G3	Stage IIIA	T3	M0	N0
TCGA-CC-5264	71	MALE	G2	Stage IIIA	T3	M0	N0
TCGA-ED-A8O6	50	FEMALE	G3	Stage IIIA	T3a	M0	N0
TCGA-DD-A115	53	MALE	G2	Stage IIIA	T3	M0	N0
TCGA-BW-A5N0	50	MALE	G2	Stage IIIA	T3a	MX	NX
TCGA-CC-A5UD	45	MALE	G2	Stage IIIA	T3	M0	N0
TCGA-CC-A9FU	52	FEMALE	G2	Stage IIIA	T3a	M0	N0
TCGA-FV-A4ZP	78	MALE	G2	Stage IIIA	T3	M0	NX
TCGA-CC-A7IE	57	MALE	G2	Stage IIIA	T3	M0	N0
TCGA-CC-A1HT	50	MALE	G3	Stage IIIA	T3	M0	N0

Table 1 continued. The clinical characteristics of patients with hepatocellular carcinoma.

Id	Age	Gender	Grade	Stage	T	M	N
TCGA-CC-A7IL	61	MALE	G1	Stage IIIA	T3	M0	NO
TCGA-CC-5263	35	MALE	G1	Stage IIIA	T3	M0	NO
TCGA-DD-A4NV	61	MALE	G1	Stage IIIA	T3	M0	NO
TCGA-DD-A4NK	80	FEMALE	G2	Stage IIIA	T3	M0	NO
TCGA-CC-A9FW	68	MALE	G2	Stage IIIA	T3	M0	NO
TCGA-CC-A8HU	39	FEMALE	G3	Stage IIIA	T3	M0	NO
TCGA-UB-A7MF	56	MALE	G2	Stage IIIA	T3a	MX	NX
TCGA-ED-A66Y	51	FEMALE	G3	Stage IIIA	T3a	M0	NO
TCGA-DD-A116	68	MALE	G3	Stage IIIA	T3	M0	NO
TCGA-CC-A9FV	57	MALE	G2	Stage IIIA	T3	M0	NO
TCGA-CC-A3MC	54	MALE	G2	Stage IIIA	T3	M0	NO
TCGA-CC-A123	24	FEMALE	G1	Stage IIIA	T3	M0	NO
TCGA-XR-A8TE	16	MALE	G1	Stage IIIA	T3	MX	NO
TCGA-CC-A8HT	74	MALE	G2	Stage IIIA	T3	M0	NO
TCGA-DD-AADG	70	MALE	G3	Stage IIIA	T3a	M0	NO
TCGA-2Y-A9H0	49	MALE	G1	Stage IIIA	T3	M0	NO
TCGA-G3-AAV6	53	FEMALE	G3	Stage IIIA	T3a	M0	NO
TCGA-DD-A4NE	75	FEMALE	G3	Stage IIIA	T3a	M0	NO
TCGA-ED-A7XO	29	MALE	G2	Stage IIIA	T3a	M0	NO
TCGA-EP-A3RK	73	MALE	G2	Stage IIIA	T3a	MX	NX
TCGA-BC-4072	74	FEMALE	G3	Stage IIIA	T3	M0	NO
TCGA-ED-A82E	60	FEMALE	G2	Stage IIIA	T3a	M0	NO
TCGA-BC-A5W4	69	MALE	G3	Stage IIIA	T3a	M0	NX
TCGA-CC-A3MB	36	MALE	G1	Stage IIIA	T3	M0	NO
TCGA-G3-A25T	45	FEMALE	G2	Stage IIIA	T3	M0	NO
TCGA-G3-A3CH	53	MALE	G2	Stage IIIA	T3a	M0	NO
TCGA-BC-4073	73	MALE	G3	Stage IIIA	T3	MX	NO
TCGA-DD-A4NG	77	MALE	G2	Stage IIIA	T3a	M0	NX
TCGA-DD-AAVY	56	MALE	G2	Stage IIIA	T3	M0	NO
TCGA-CC-A7IK	59	MALE	G3	Stage IIIA	T3	M0	NO
TCGA-ED-A805	59	FEMALE	G3	Stage IIIA	T3a	M0	NO
TCGA-ED-A66X	35	MALE	G3	Stage IIIA	T3a	M0	NO
TCGA-BC-A10X	52	FEMALE	G2	Stage IIIA	T3a	MX	NO
TCGA-LG-A9QD	68	MALE	G2	Stage IIIA	T3a	M0	NO
TCGA-WX-AA47	33	FEMALE	G2	Stage IIIA	T3a	MX	NX

Table 1 continued. The clinical characteristics of patients with hepatocellular carcinoma.

Id	Age	Gender	Grade	Stage	T	M	N
TCGA-NI-A4U2	71	MALE	G1	Stage IIIA	T3	MX	NX
TCGA-BC-A216	62	FEMALE	G2	Stage IIIA	T3	M0	NX
TCGA-CC-A7IH	58	MALE	G1	Stage IIIA	T3	M0	N0
TCGA-YA-A8S7	68	MALE	G3	Stage IIIA	T3a	MX	N0
TCGA-DD-A1EE	73	MALE	G3	Stage IIIA	T3	M0	N0
TCGA-RC-A6M4	74	FEMALE	G2	Stage IIIA	T3	MX	NX
TCGA-DD-AAD6	66	MALE	G3	Stage IIIA	T3a	M0	N0
TCGA-CC-A3MA	61	MALE	G2	Stage IIIA	T3	M0	N0
TCGA-DD-A3A1	65	MALE	G2	Stage IIIA	T3b	M0	N0
TCGA-5R-AA1D	17	FEMALE	G3	Stage IIIA	T3a	M0	N0
TCGA-CC-A5UE	48	MALE	G2	Stage IIIB	T4	M0	N0
TCGA-G3-A6UC	65	MALE	G2	Stage IIIB	T3b	M0	N0
TCGA-PD-A5DF	58	FEMALE	G2	Stage IIIB	T4	M0	N0
TCGA-DD-A4NH	65	FEMALE	G3	Stage IIIB	T3b	M0	N0
TCGA-3K-AAZ8	65	MALE	G1	Stage IIIB	T3b	MX	NX
TCGA-XR-A8TD	49	FEMALE	G3	Stage IIIB	T3	M0	N0
TCGA-G3-A25W	79	FEMALE	G2	Stage IIIB	T3b	M0	N0
TCGA-DD-A3A7	67	MALE	G3	Stage IIIB	T3b	M0	N0
TCGA-G3-A7M9	70	MALE	G2	Stage IIIB	T3b	MX	NX
TCGA-CC-5259	60	FEMALE	G2	Stage IIIC	T4	M0	N0
TCGA-BC-A8YO	66	FEMALE	G3	Stage IIIC	T4	M0	N0
TCGA-CC-5262	67	MALE	G1	Stage IIIC	T4	M0	N0
TCGA-DD-A4NA	67	FEMALE	G3	Stage IIIC	T2	M0	N1
TCGA-MI-A75E	61	MALE	G2	Stage IIIC	T4	M0	N0
TCGA-G3-AAV1	51	MALE	G3	Stage IIIC	T4	M0	N0
TCGA-CC-5260	61	FEMALE	G1	Stage IIIC	T4	M0	N0
TCGA-DD-A1EJ	71	FEMALE	G2	Stage IIIC	T1	M0	N1
TCGA-CC-A8HS	18	MALE	G1	Stage IIIC	T3	M0	N1
TCGA-DD-A119	40	MALE	G3	Stage IV	T3a	M1	N0
TCGA-BW-A5NP	26	FEMALE	G3	Stage IV	T2	M1	N0
TCGA-RC-A6M5	20	FEMALE	G2	Stage IVA	T1	M0	N1
TCGA-DD-A1EK	64	FEMALE	G2	Stage IVB	T4	M1	N0
TCGA-DD-A3A9	64	FEMALE	G2	Stage IVB	T4	M1	N0

The single-cell sequencing data included biospecimens from 9 patients with HCC and 10 patients with intrahepatic cholangiocarcinoma. This dataset delineates the single-cell transcriptomic landscape of liver cancer samples from 19 patients, providing valuable insights into the TME of HCC. We extracted a total of 434 ARGs from GeneCards (<https://www.genecards.org/>) and selected 61 genes with correlation scores greater than 2.

Single-Sample Gene Set Enrichment Analysis

The single-sample gene set enrichment analysis (ssGSEA) method enables enrichment analysis of samples based on a given gene set, providing enrichment scores. This allowed us to compare the enrichment status of the given gene set between different groups [28]. We used the GSEA (version 1.50.0), limma (version 3.58.1), and GSEABase (version 1.64.0) packages in R to compute the enrichment scores for ARG score, immune cells, and immune function in the HCC transcriptome data. GSEA and GSEABase offer greater capability to detect subtle pathway activity changes within sample populations [29,30]. The limma package is an R/Bioconductor software package that provides an integrated solution for analyzing data from gene expression experiments [31]. Based on the median value of ARG scores, we divided the HCC samples into high-ARG-score and low-ARG-score groups. To compare the differences in immune cells and immune function between the 2 groups, we used the limma, reshape2 (version 1.4.4), and ggpubr (version 0.6.0) packages in R [32]. The reshape2 and ggpubr packages assisted us in visualizing the results. Additionally, we used the Estimation of Stromal and Immune cells in Malignant Tumor tissues using Expression data (ESTIMATE) algorithm to evaluate the immune and stromal scores between the low-ARG-score and high-ARG-score groups [33].

Identification of ARG-Related lncRNAs

We conducted univariate Cox regression analysis to investigate the relationship between 61 ARGs and the survival of HCC patients, identifying 24 ARGs significantly associated with HCC prognosis ($P < 0.05$). Subsequently, we used a stringent criterion, utilizing the Wilcoxon rank sum test ($\text{corFilter} = 0.6$, $\text{pvalueFilter} = 0.001$), to screen for lncRNAs highly correlated with ARGs. This rigorous standard helped us attain more relevant genes. Additionally, we analyzed whether the screened lncRNAs exhibited differential expression levels in HCC and were associated with patient prognosis. Ultimately, we identified 34 genes highly correlated with ARGs, differentially expressed in HCC, and associated with patient prognosis.

Construction of the Risk Model

To mitigate the risk of overfitting, we used the Least Absolute Shrinkage and Selection Operator (LASSO) Cox regression model

via the glmnet R package (version 4.1-8) [34,35]. In addition to providing the patient's gene expression, TCGA's liver cancer data provides the corresponding patient's survival time and survival status. We standardized the HCC data and extracted the expression levels of 34 lncRNAs for integration with survival data into a unified table, serving as the input for LASSO analysis (**Supplementary Table 1**). The lncRNAs signature was derived as follows: $\text{lncRNAs risk score} = \sum (\beta_i \times \text{Exp}_i)$, where β_i denotes the LASSO coefficient of the i -th gene, and Exp_i represents the expression value of the i -th candidate gene. It is well-established that LASSO regression effectively eliminates redundant variables by penalizing regression coefficients based on parameter size. We used the LASSO regression method for feature selection and constructing prediction signatures. LASSO regression attenuates coefficient estimates toward zero, contingent on the regularization parameter λ [36]. To ascertain the optimal λ , we used 10-fold cross-validation and selected λ based on the minimum criterion. Subsequently, patients were stratified into high and low lncRNAs risk groups according to the median lncRNAs score, and their association with overall survival was assessed using Kaplan-Meier analysis. We used the pheatmap package (version 1.0.12) to visually represent the obtained lncRNA signature in the form of a heatmap. Furthermore, we generated a receiver operating characteristic (ROC) curve employing the timeROC package (version 0.4) and evaluated its accuracy using the area under the curve (AUC) model [37].

Risk Model and Clinical Features of HCC

We evaluated the relationship between the risk score and the clinical characteristics of HCC patients, including age, sex, disease stage, and grade, using univariate and multivariate regression analysis. Additionally, we used the rms package (version 6.7-1) and survival package (version 3.5-7) to draw column diagrams and 1-year, 3-year, and 5-year calibration curves to further analyze the risk model and HCC clinical characteristics.

Infiltration of Immune Cells

To quantify the relative proportions of infiltrating immune cells, we used various methods, such as TIMER, CIBERSORT, CIBERSORT-ABS, QUANTISEQ, MCPCOUNTER, XCELL, and EPIC [38]. CIBERSORT and CIBERSORT-ABS are versatile computational methods used to quantify the cellular composition of large-scale tissue gene expression profiles, enabling accurate estimation of the immune composition of tumor biopsies [39,40]. QUANTISEQ, XCELL, EPIC, and MCPCOUNTER are computational pipelines for quantifying immune cell fractions from bulk RNA sequencing data obtained from blood or tumor samples [41-43]. These methods are commonly used for quantifying immune cell content in RNA-seq data [40,44]. The TIMER database (<https://cistrome.shinyapps.io/timer/>), which comprises 10 897 samples across 32 cancer types from TCGA, was used to

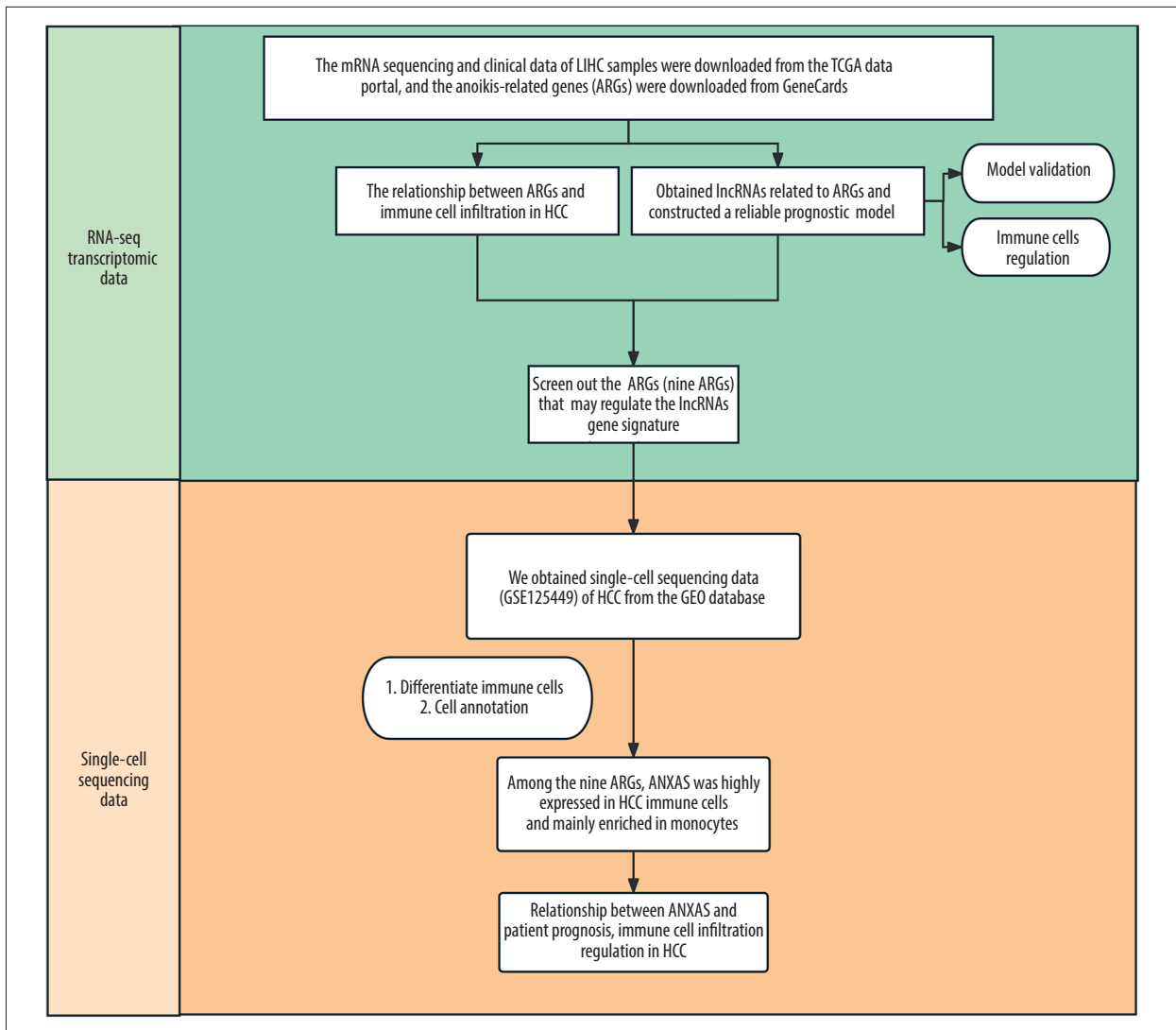


Figure 1. The detailed flow chart of this study.

analyze the level of tumor-associated immune cell infiltration in the TME [45]. Additionally, we used TIMER to investigate the correlation between genes and immune cell infiltration. Based on the data obtained from the Human Protein Atlas (<https://www.proteinatlas.org/>), the hub gene was considered as a novel biomarker of HCC. We used the pheatmap package (version 1.0.12) to visually represent the quantified immune cells mentioned above in the form of a heatmap. From published literature, we gathered 39 common immune checkpoints for subsequent analysis [46]. Using the ggplot2 package (version 3.4.4) and limma package, we visualized the differences in cell types and immune checkpoints between different groups through boxplots.

Single-Cell Data Processing and Dimensionality Reduction

To process the single cell data, we used the Seurat package (version 5.0.1) within R software [47]. The Seurat package is the

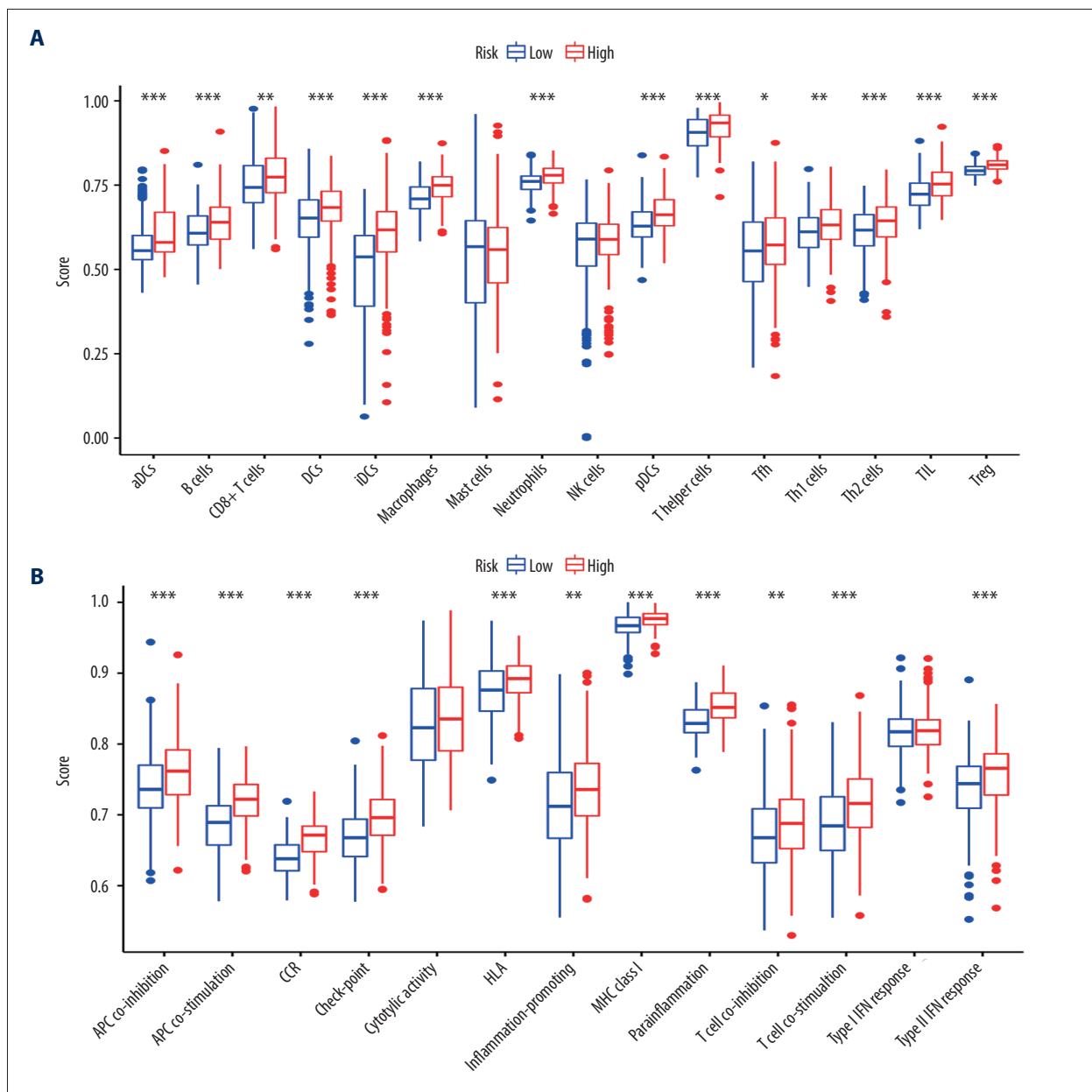
most commonly used method for analyzing single-cell data, encompassing functionalities such as data importation, filtering, normalization, feature selection, scaling, dimensionality reduction, clustering, data visualization, and differential gene expression analysis [48-50]. Due to limitations in sequencing depth and inherent gene expression levels, single-cell sequencing data often present a matrix with numerous “0” values, a phenomenon referred to as “drop-out”. These zeros can result from insufficient sequencing depth preventing gene capture or from genes not being expressed. Normal cell gene expression levels typically range from 3000 to 4000. Additionally, cells with fewer detected genes, low count depth, and a high proportion of mitochondrial counts are often deemed low-quality cells, as they can represent dying or ruptured membrane cells [51]. The gene and count features were identified for each sample, and cells with less than 300 or more than 7000 features were filtered out. Additionally, cells with a mitochondrial RNA percentage

greater than 10 or ribosome RNA percentage less than 3 were removed. The samples were integrated using the merge function and underwent normalized, scaled, and principal component analysis. To address any potential batch effects within subgroups, we used the harmony package (version 1.2.0) [49]. The FindAllMarkers function was used to identify the marker genes of each cluster. Finally, dimensionality reduction clustering was performed on the resulting dataset using UMAP. Given our primary focus on immune cells, we used the immune cell marker PTPRC to distinguish cells into immune and non-immune categories. Subsequently, immune cells were extracted for separate clustering and cell annotation using SingleR (version 2.4.1). SingleR assigns cellular identities to single-cell transcriptomes

by comparing them to reference datasets of pure cell types sequenced via microarray or RNA-seq [52]. We quantified the expression levels of monocytes in HCC samples using the ssGSEA method and analyzed the relationship between monocyte content in samples and patient prognosis using the survival package (version 3.5-7). We quantified the level of monocyte infiltration using the ssGSEA method and analyzed the impact of ANXA5 and monocytes on HCC patient prognosis.

Statistics

R software (version 4.1.3, <https://www.r-project.org/>) and associated R packages were used to perform all graphical and



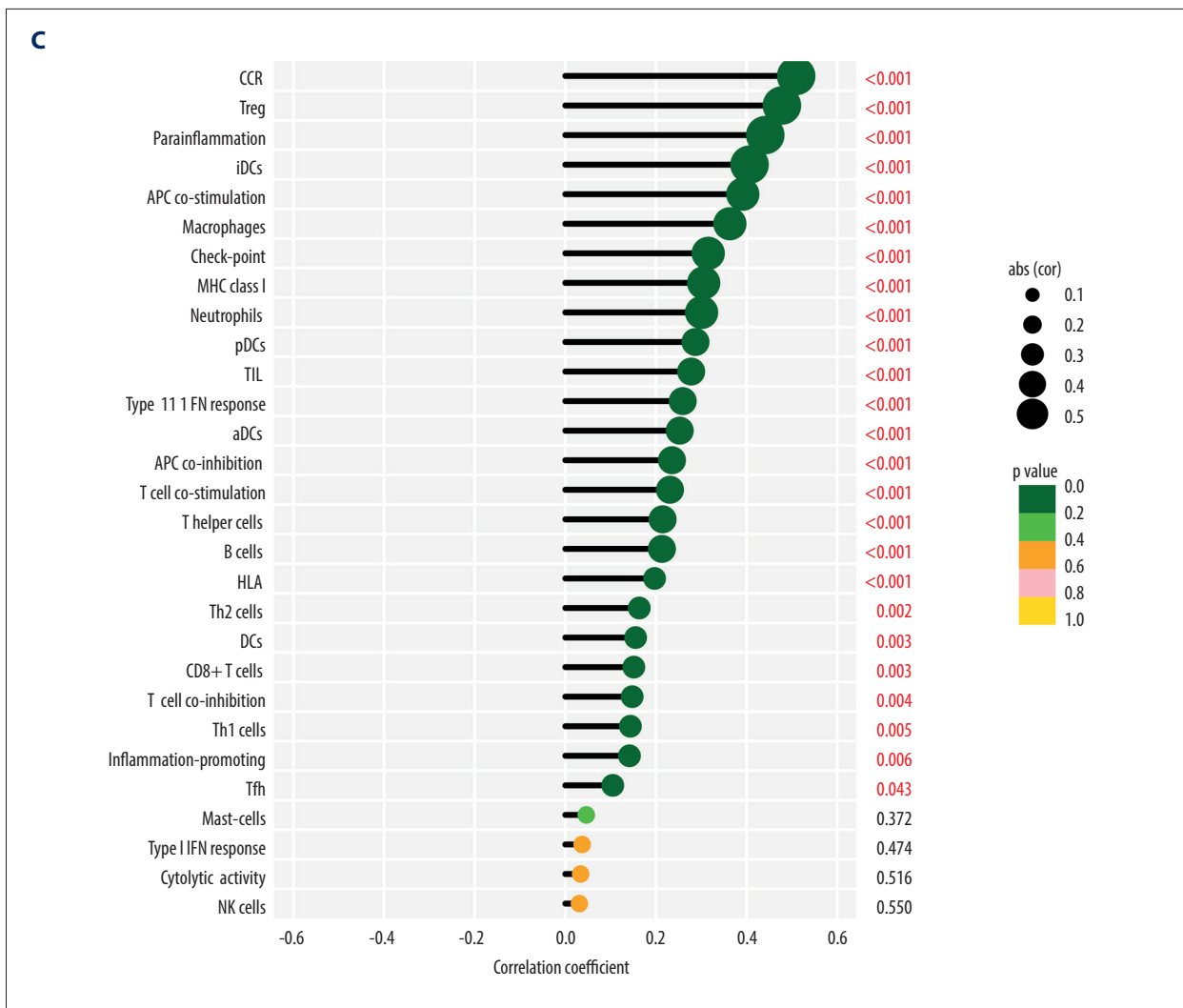


Figure 2. Relationship between anoikis-related genes (ARGs) and hepatocellular carcinoma (HCC) immune cells and immune function. (A) Boxplot showing the difference in immune cell infiltration level between the high and low ARGs score groups. **(B)** Boxplot showing the difference in immune function between the high and low ARGs score groups. **(C)** Correlation between ARGs expression and immune cell infiltration and immune function in HCC samples. (* $P < 0.05$, ** $P < 0.01$, *** $P < 0.001$, ns: no significance).

statistical analyses. The *t* test was used to compare the differences between 2 groups of samples. Survival analysis was performed using the log-rank test. $P < 0.05$ was considered statistically significant.

Results

Relationship between ARGs and Immune Infiltration in HCC

The research process outline is shown in **Figure 1**. Following the methods outlined in the section “Single-sample gene set enrichment analysis,” we scored the expression levels of 61

ARGs in HCC samples. We used the ssGSEA method to assess the expression levels of ARGs in HCC samples and categorized them into low- and high-ARG-score groups based on the median. Additionally, using the approach described in the section “Infiltration of immune cells,” we quantified the immune cell populations and functions within HCC samples. To assess the relationship between ARGs and immune cell infiltration, we compared the differences in immune cell composition and function between the 2 sample groups (**Figure 2A, 2B**). Our findings revealed that the high-ARG-score group had increased immune cell infiltration and immune function scores. Furthermore, correlation analysis indicated a positive correlation between ARG score and immune cell infiltration and function in HCC samples (**Figure 2C**).

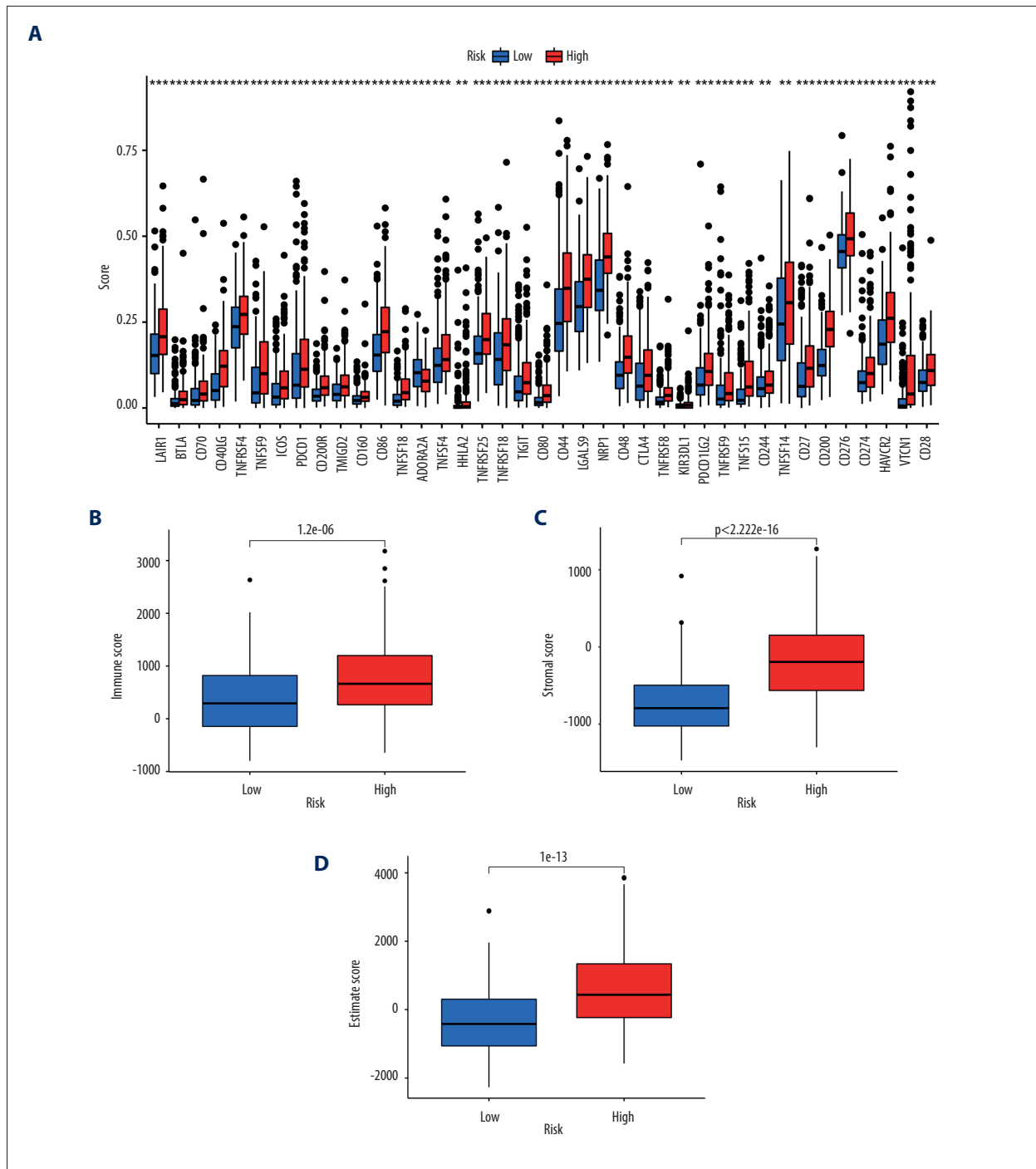


Figure 3. The relationship between ankiis-related genes (ARGs) score and immune cell infiltration in hepatocellular carcinoma (HCC) samples. **(A)** Box plot of differences in immune checkpoints between high ARGs score group and low ARGs score groups. **(B-D)** The differences in StromalScore, ImmuneScore, and ESTIMATEScore between the high and low ARGs score groups. (* $P < 0.05$, ** $P < 0.01$, *** $P < 0.001$, ns – no significance).

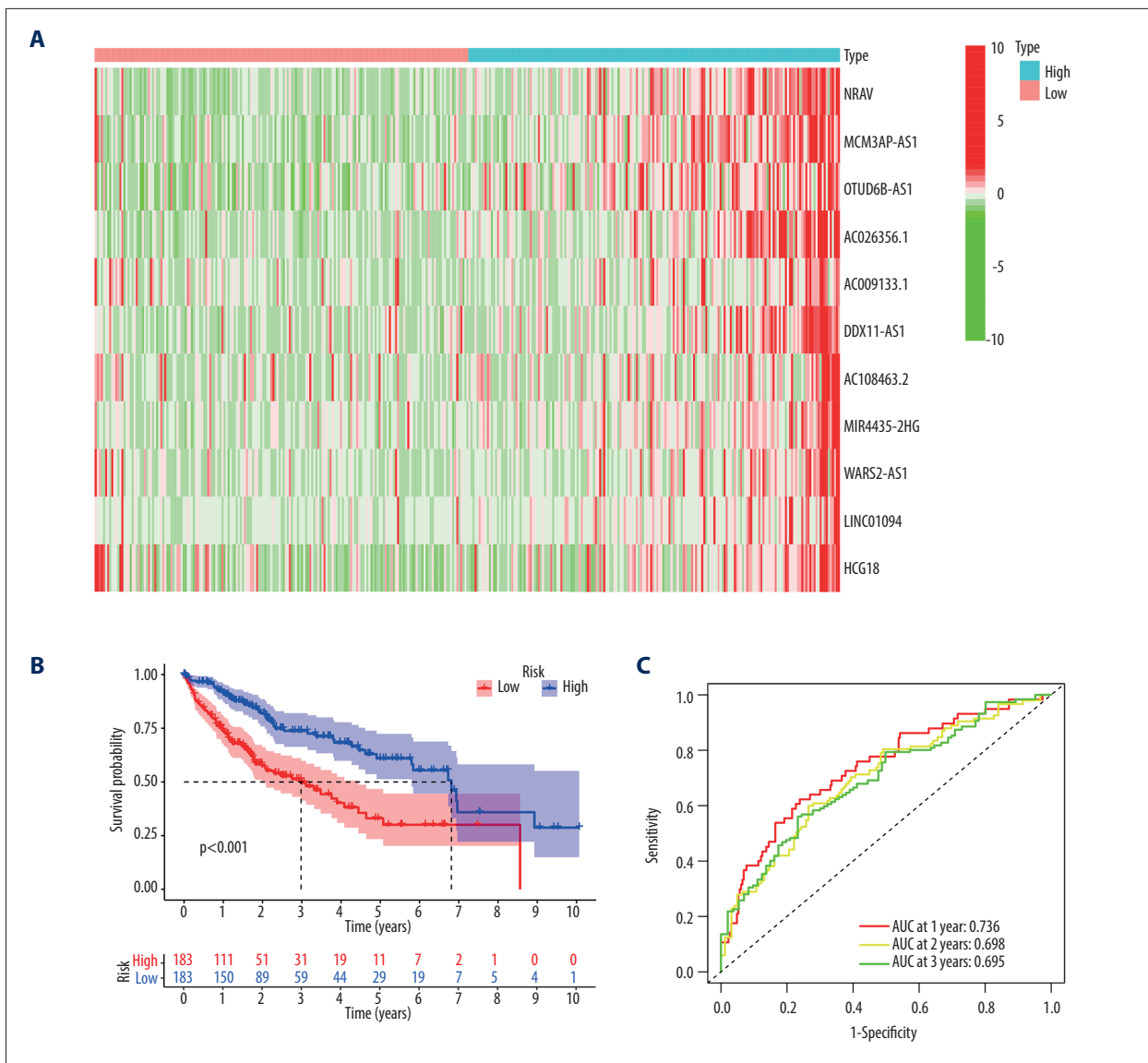


Figure 4. Construction of the prognostic model of anoikis-related genes (ARG-related lncRNAs). (A) Heat map of the expression levels of 11 long non-coding RNAs (lncRNAs) in high-risk group and low-risk group samples for constructing the prognosis model. (B) Survival curves of high-risk group samples and low-risk group samples. (C) ROC curve to show the accuracy of the model.

Relationship Between ARGs and Immune Cells

Immune checkpoint blockade therapy targeting immune checkpoints can inhibit negative regulation signal transduction and alleviate T-cell exhaustion [53]. Consequently, immune checkpoint blockade therapy can reverse the immunosuppressive microenvironment and reduce the probability of tumor immune escape, thus improving the prognosis [54]. Given the close relationship between ARG expression level and HCC immune cell infiltration and immune function, we further evaluated the connection between ARGs and immune checkpoints (Figure 3A). We then compared the differences in immune indices, including StromalScore ($P < 2.22e-16$), ImmuneScore

($P < 1.2e-06$), and ESTIMATEScore ($P < 1e-13$) between the high- and low- ARG-score groups (Figure 3B-3D). Our findings indicated that the high-ARG-score group exhibited increased expression levels of immune checkpoints and higher immune indices, which implies improved immune efficacy.

ARG-Related lncRNAs

To gain a comprehensive understanding of the role of ARGs in HCC, we identified 24 prognosis-related ARGs and selected 33 lncRNAs related to ARGs. The screening criteria for lncRNAs were correlation > 0.6 , P value < 0.001 . From these 33 lncRNAs, we selected 11 lncRNAs (NRAV, MCM3AP-AS1, OTUD6B-AS1,

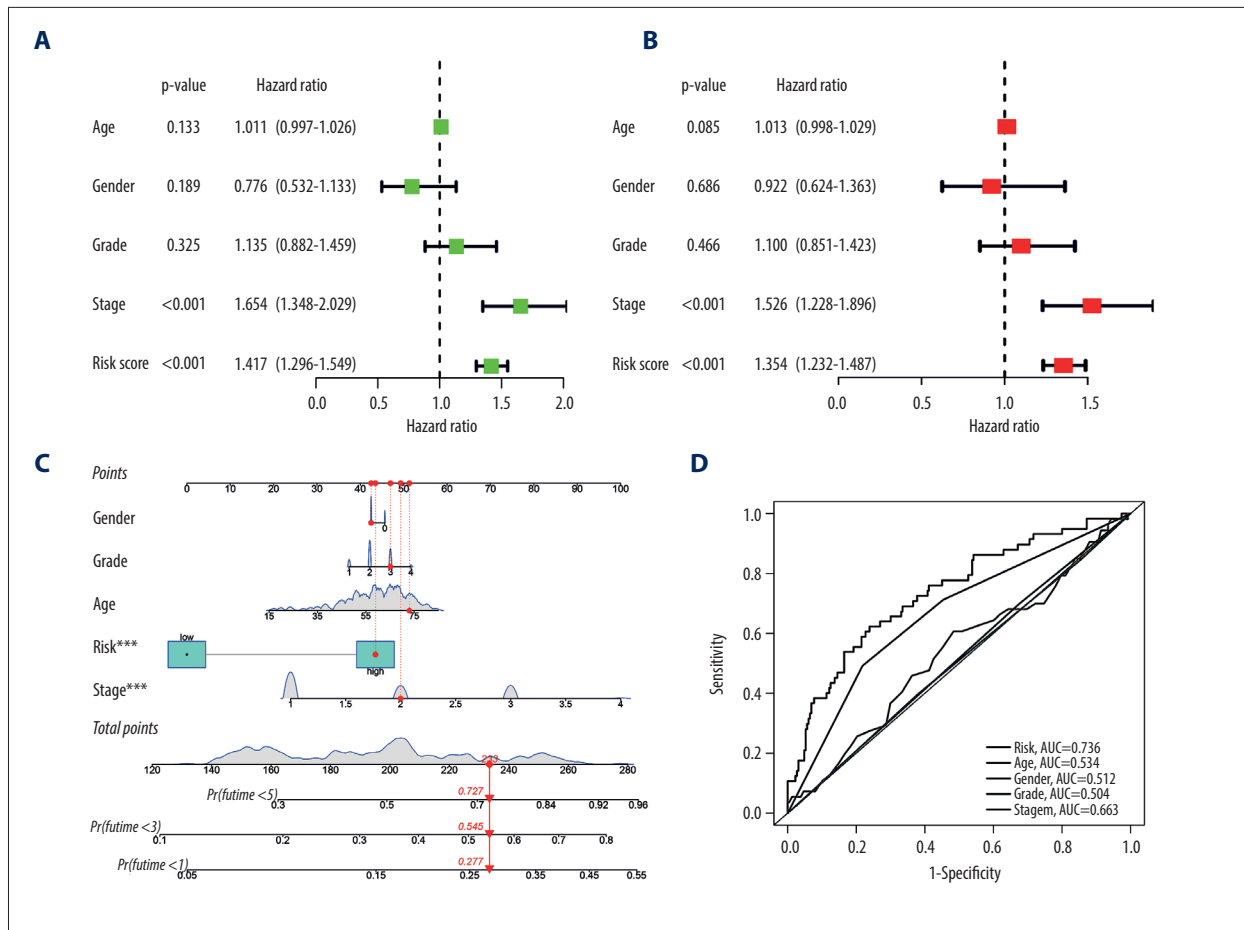


Figure 5. Evaluation of the prognostic model. (A, B) Univariate and multivariate COX regression analyzes to study the relationship between risk score and patient outcome. (C) A nomogram was drawn to show the relationship between the risk model and patient outcomes. (D) ROC curve to evaluate the accuracy of each indicator in the nomogram model.

AC026356.1, AC009133.1, DDX11-AS1, AC108463.2, MIR4435-2HG, WARS2-AS1, LINC01094, and HCG18) and constructed a COX risk model. The heatmap (Figure 4A) showed the differential expression of these 11 lncRNAs between the high-risk and low-risk groups, with higher expression levels in the high-risk group. The prognostic analysis based on the risk model revealed that patients in the low-risk group had a better survival status (Figure 4B; $P < 0.001$). Furthermore, the area under the ROC curve (AUC) for 1 year, 3 years, and 5 years of overall survival were all greater than 0.65, indicating the model's reliability (Figure 4C; AUC at 1 year: 0.736; AUC at 3 years: 0.698; AUC at 5 years: 0.695).

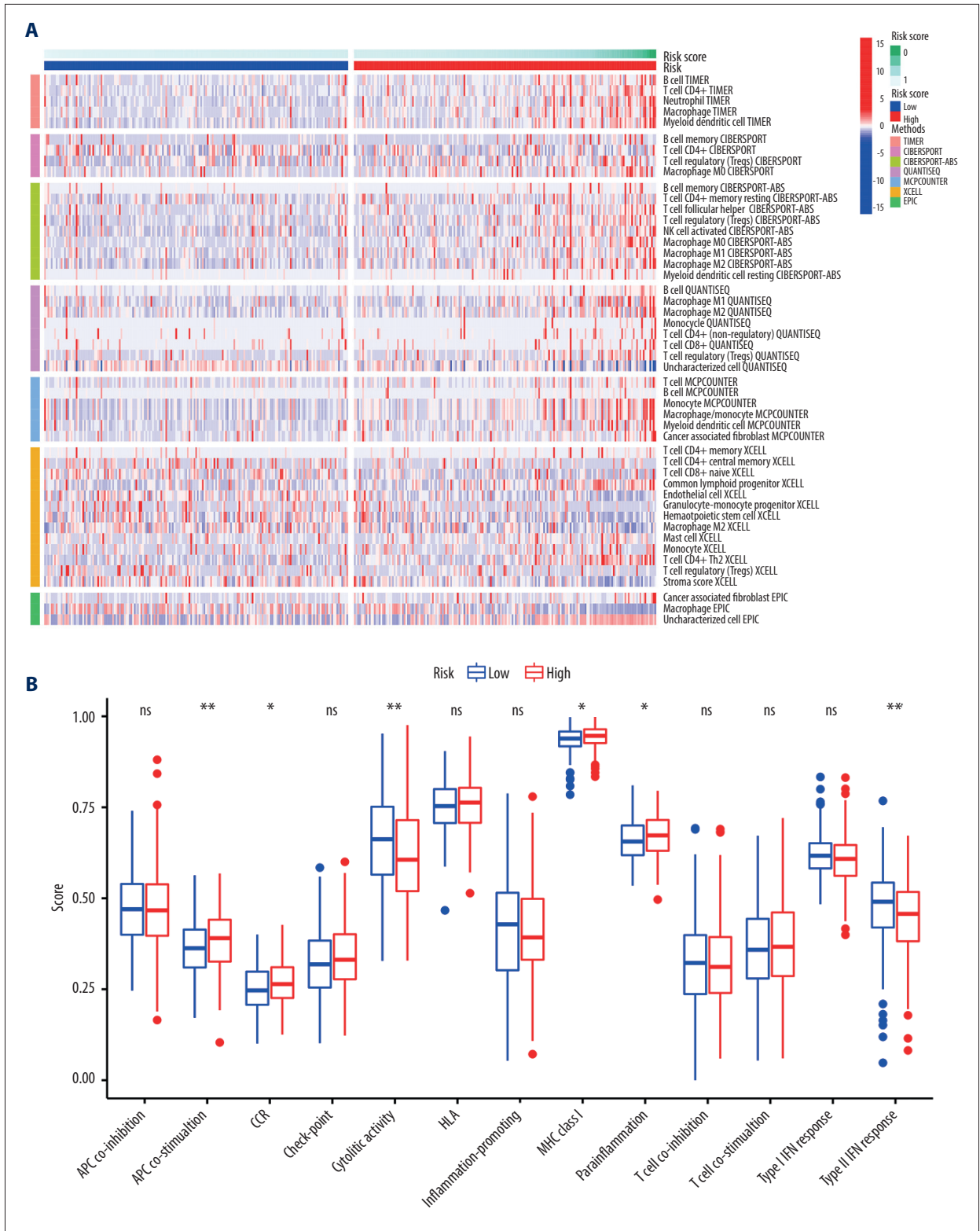
Prognostic Model Evaluation

We also performed univariate and multivariate COX regression analyses and found that risk score and stage were associated with the prognosis of HCC patients (Figure 5A, 5B; risk score < 0.001). We developed a nomogram for HCC patients that incorporated multiple clinical factors and risk scores and

validated its accuracy using a ROC curve (risk, AUC=0.736). The results demonstrated that risk score and stage were important factors for HCC prognosis, and the ROC curve confirmed the model's accuracy (Figure 5C, 5D).

Risk Model and Immune Infiltration

In terms of the risk model and immune infiltration, we utilized the TIMER, CIBERSORT, CIBERSORT-ABS, QUANTISEQ, MCPOUNTER, XCELL, and EPIC methods to evaluate the relative proportions of infiltrating immune cells. The results showed that the high-risk group had higher levels of immune cell infiltration (Figure 6A). Additionally, we compared the differences in immune cell composition and function between the 2 sample groups (Figure 6B, 6C). The results indicated that the high-risk group had higher levels of immune cell infiltration, immune function scores, and expression of immune checkpoint genes, suggesting a better response to immunotherapy.



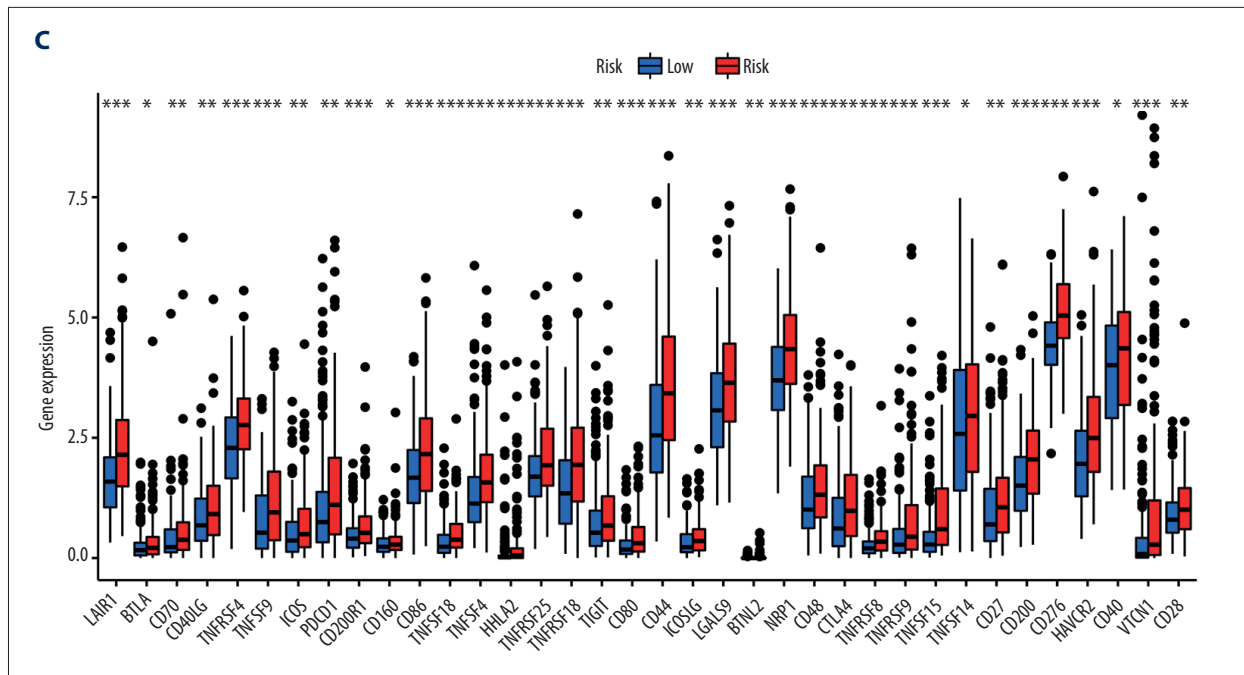


Figure 6. Relationship between risk model and immune infiltration. (A) TIMER, CIBERSORT, CIBERSORT-ABS, QUANTISEQ, MCPOUNTER, XCELL, and EPIC methods to evaluate the relative proportions of infiltrating immune cells. (B) Differences in immune function between high-risk and low-risk samples. (C) Differences in expression levels of immune checkpoints between high-risk and low-risk samples. (* $P < 0.05$, ** $P < 0.01$, *** $P < 0.001$, ns – no significance)

ANXA5 and Immune Cells in HCC

We identified 11 lncRNAs used to construct the risk model, of which 4 showed a high correlation with ANXA5, suggesting its crucial role in HCC (Figure 7A). To investigate the relationship between ANXA5, immune cells, and patient prognosis in HCC, we analyzed single-cell sequencing data. Based on CD45 expression, we classified cells into immune and non-immune cells and extracted immune cells to annotate ARGs (Figure 7B-7D). ANXA5 showed the highest expression level among the 9 ARGs related to the risk model in single cells, primarily in monocytes, as indicated by FCGR3A and CD14 (Figure 8A, 8B).

Relationship Between ANXA5 and Immune Cell Infiltration in HCC

We quantified the level of monocyte infiltration using the ssGSEA method and analyzed the impact of ANXA5 and monocytes on HCC patient prognosis. We found that higher levels of monocyte infiltration were associated with better prognosis, while increased ANXA5 expression was associated with worse prognosis ($P < 0.05$; Figure 9A, 9B). ANXA5 and monocyte infiltration may have a synergistic effect on HCC prognosis ($P < 0.001$; Figure 9C). In the TIMER database, ANXA5 was negatively correlated with CD14 ($r = -0.152$, $P = 3.35 \times 10^{-3}$) but positively correlated with FCGR3A ($r = 0.493$, $P = 4.29 \times 10^{-24}$). ANXA5 was also negatively correlated with tumor purity

($r = -0.322$, $P = 8.95 \times 10^{-10}$) but positively correlated with monocytes ($r = 0.548$, $P = 1.93 \times 10^{-28}$; Figure 9D).

Discussion

HCC is a prevalent malignancy worldwide with high mortality rates. In recent years, targeted agents, such as sorafenib, lenvatinib, and regorafenib, have shown promising benefits in treating metastatic or unresectable HCC. Despite advancements in therapy, the overall survival of patients with advanced HCC remains unsatisfactory [55]. However, immunotherapy has emerged as a promising treatment option for inhibiting tumor progression and even preventing relapse [56-58]. The identification of reliable and effective biomarkers for HCC prognosis is of the utmost importance. To provide insights for personalized treatment of HCC patients, we conducted a comprehensive investigation of the relationship between ARGs and immune cells in HCC.

Our initial investigation focused on exploring the association between ARGs and immune cell infiltration in HCC. Our findings revealed that samples with high expression of ARGs exhibited increased levels of immune cell infiltration, including T cells, B cells, and macrophages, and expression of immune checkpoint genes, such as PDCD1. TAMs are associated with poor prognosis in head and neck squamous cell carcinoma.

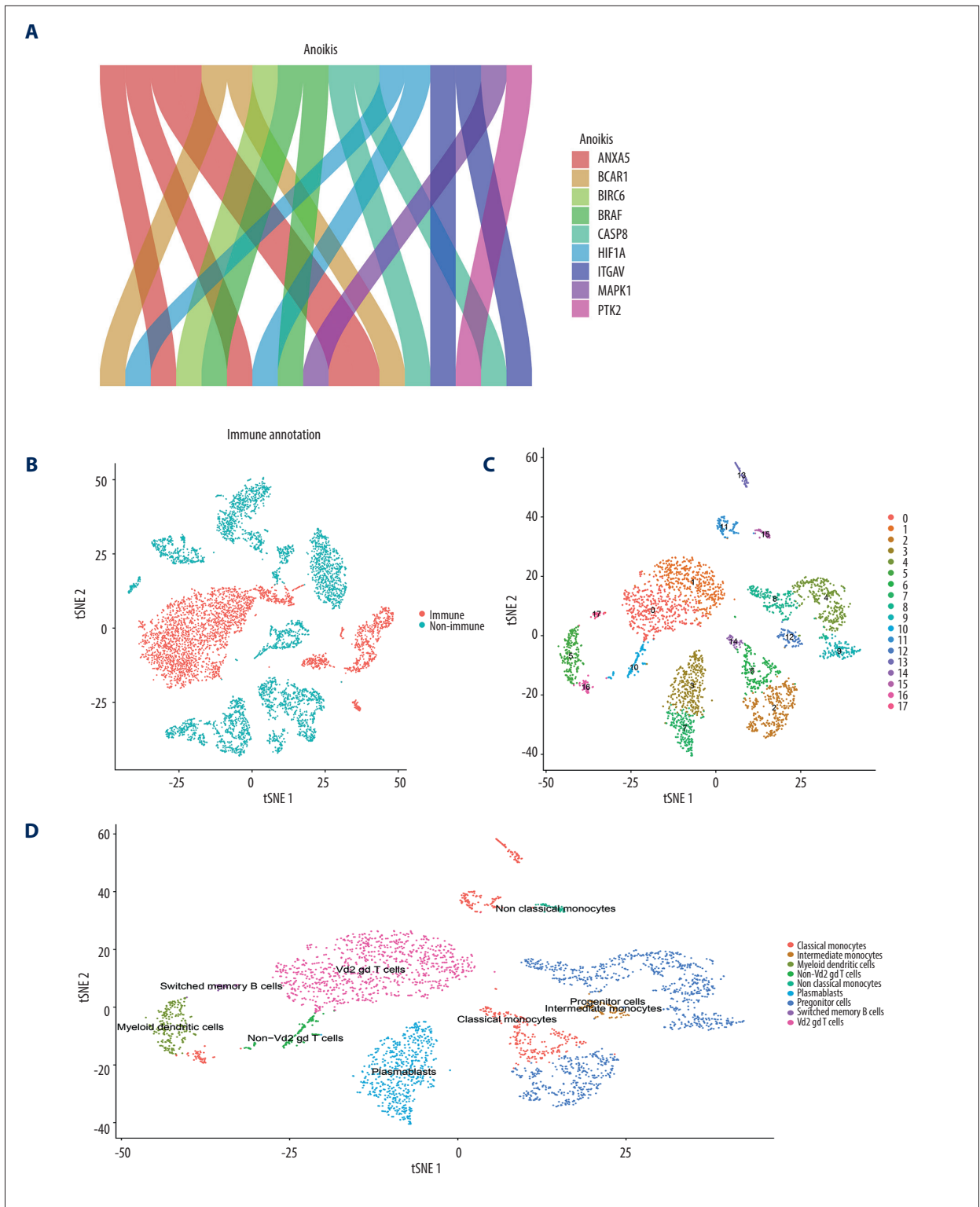


Figure 7. ANXA5 and immune cells in hepatocellular carcinoma (HCC). **(A)** Mulberry plot to show the relationship of the 9 anoikis-related genes (ARGs) with the 11 long non-coding RNAs (lncRNAs) that constitute the risk model. **(B-D)** Annotated map of immune cell clustering.

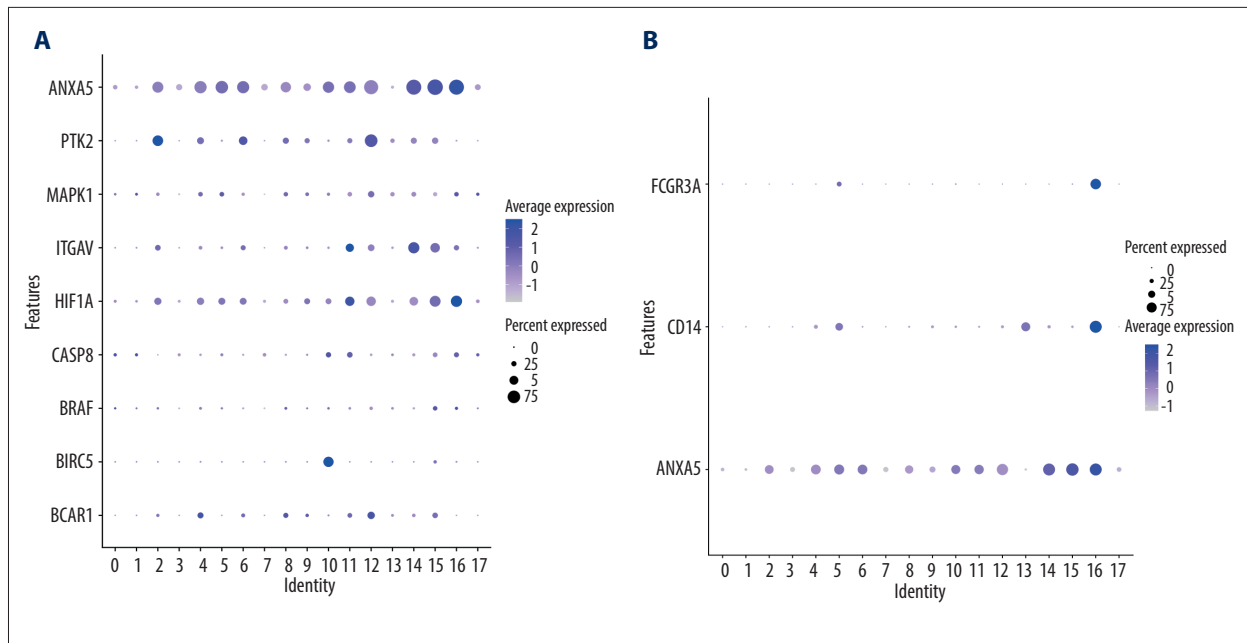


Figure 8. ANXA5 and monocytes. (A) Bubble plot of the expression of 9 anoikis-related genes (ARGs) in different classes of immune cells associated with the risk model. (B) Bubble plot of expression levels of ANXA5 and monocyte markers FCGR3A and CD14.

TAMs, derived from inflammatory monocytes, play a crucial role in regulating tumor progression. Generally, TAMs promote tumor progression [59]. The coordinated immune response of regulatory T lymphocytes, helper T lymphocytes, and cytotoxic T lymphocytes significantly influences the progression from chronic liver disease to HCC [60-62]. Particularly, cytotoxic T cells play a crucial role in clearing infections or malignant liver cells [63]. This implies that the high expression of ARGs may promote the prognosis of HCC patients receiving immune therapy by enhancing the secretion of TAMs and cytotoxic T cells. Higher expression of the immune checkpoint PD-1 is significantly correlated with shorter overall survival and later tumor staging in patients with cancer [64]. PD-1 leads to T-cell exhaustion, thereby enhancing the growth of HCC [65]. The lower proportion of PD-1+ lymphocytes is associated with better treatment response in HCC [66]. These immune checkpoints have been linked to tumor progression and clinical outcomes of tumor patients treated with immunotherapy. Increasing evidence suggests that immune checkpoint blockade can be a promising option for inoperable HCC cases [67]. Our results indicate that the expression of ARGs can be a significant factor in predicting the prognosis and potential efficacy of immunotherapy in patients with HCC. This implies that we can predict the expression of relevant immune cells and immune checkpoints based on the expression of ARGs in patients with HCC, and thus choose different treatment modalities, achieving personalized treatment for patients.

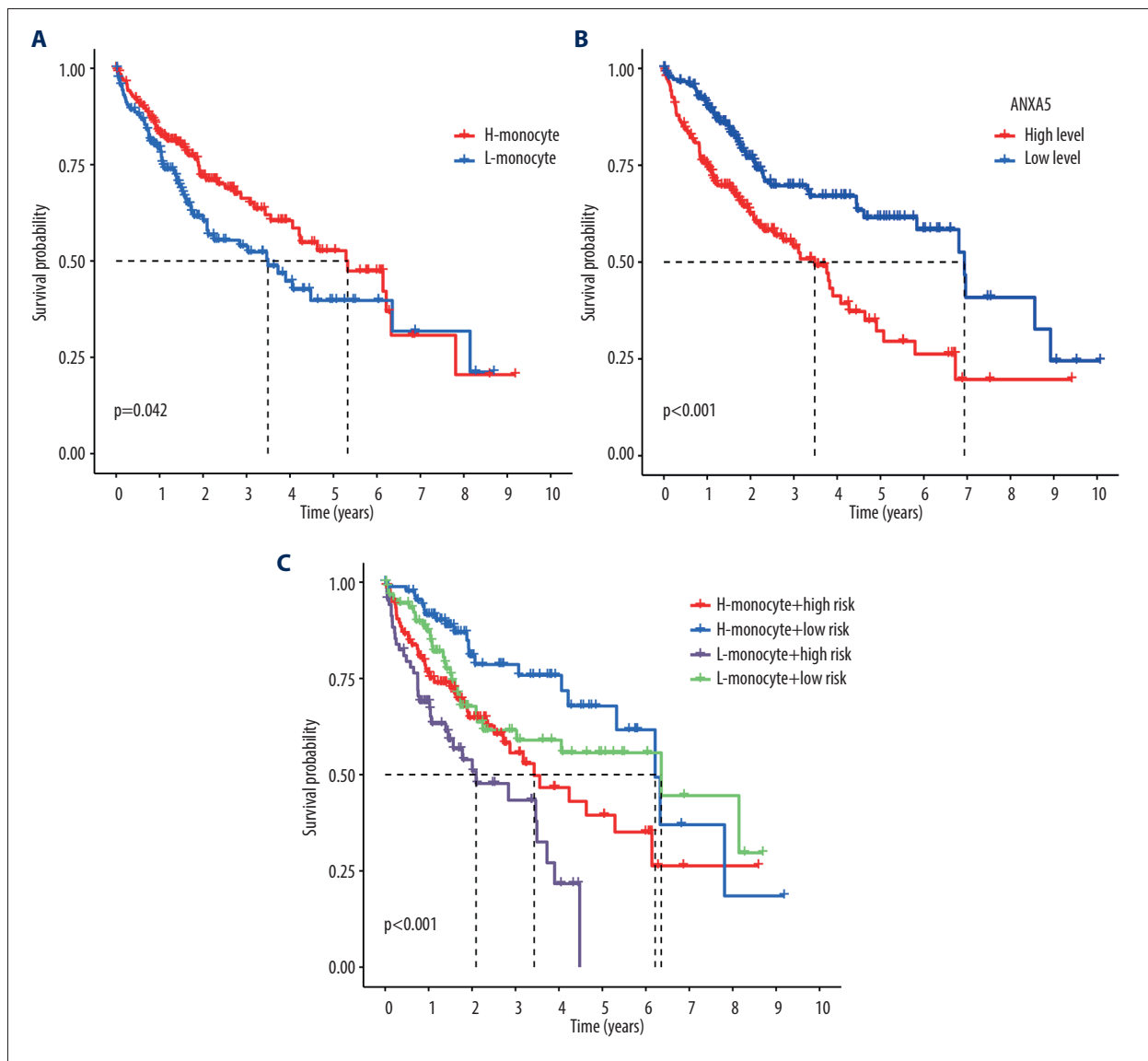
In this study, we constructed a risk model for the ARG-related lncRNAs NRAV, MCM3AP-AS1, OTUD6B-AS1, AC026356.1,

AC009133.1, DDX11-AS1, AC108463.2, MIR4435-2HG, WARS2-AS1, LINC01094, and HCG18 and examined the relationship between the model and the prognosis and immune cells of patients with HCC. Based on the median risk score, we classified the patients into 2 categories: high risk and low risk. We validated the predictive accuracy of the risk model using ROC curves and plotted a nomogram predicting HCC patient prognosis. The outcomes predicted by the model were consistent with those predicted by the nomogram. Clinicopathological analysis and survival analysis demonstrated that the model was highly sensitive to survival prediction. According to Cox regression, the model identified the prognostic factor of HCC. Utilizing this risk model in clinical practice would be beneficial by conducting risk assessment of patients with HCC based on the expression levels of ARG-related lncRNAs, thus enabling personalized treatment. Patients in the high-risk group, characterized by a robust immune response, could benefit from immunotherapy to enhance their prognosis, while those in the low-risk group could opt for alternative treatments, such as radiotherapy, chemotherapy, or targeted therapy [68].

Furthermore, our exploration of differences in the immune microenvironment between patients at low and high risk, examination of immune checkpoints, TME scores, and assessment of immune status using the ssGSEA method revealed a higher level of immune infiltration in the high-risk group. Research suggests that the level of immune infiltration is highly correlated with the efficacy of immunotherapy [69,70].

Based on the correlation between ARGs and lncRNAs, we identified ANXA5 as a potential immune modulatory factor in HCC. Analysis of single-cell data revealed widespread expression of ANXA5 in immune cells in HCC, suggesting it may serve as a new marker for tumor-associated monocytes. This implies that ANXA5 can promote the occurrence and development of HCC by regulating tumor-associated monocytes. ANXA5 is a member of the annexin family of calcium and phospholipid binding proteins, which binds with high affinity to phosphatidylserine (PS) [71]. Its preferential PS binding property has been utilized to detect cells undergoing apoptosis [72]. Moreover, studies have shown that the binding of ANXA5 to PS+ apoptotic cells can modulate the PS-mediated immunosuppressive clearance, thereby increasing the immunogenicity of apoptotic cells, including irradiated, apoptotic tumor cells [73,74]. Studies have shown that knocking out CD8 TEX-related gene ANXA5 in HCC

cell lines, among other cancer phenotypes, significantly inhibits cancer cell proliferation and migration [75]. Given that PS contributes to an immunosuppressive TME, ANXA5 can serve as a potential immune checkpoint inhibitor to enhance the immunogenicity of tumor-antigen specific immunotherapies, especially following cytotoxic chemotherapeutics [76]. Research indicates that administering ANXA5 rescues the immune-suppressive state induced by chemotherapy in the TME. Due to ANXA5's preferential homing to PS-rich tumor cells in the TME, fusing tumor antigen peptides to ANXA5 significantly enhances its immunogenicity and anti-tumor efficacy when administered after chemotherapy. Additionally, the therapeutic anti-tumor effects of ANXA5 peptide fusion can be further enhanced by administering other immune checkpoint inhibitors [77]. This suggests that targeting ANXA5 is likely to inhibit tumor cell progression by enhancing the immune function of HCC.



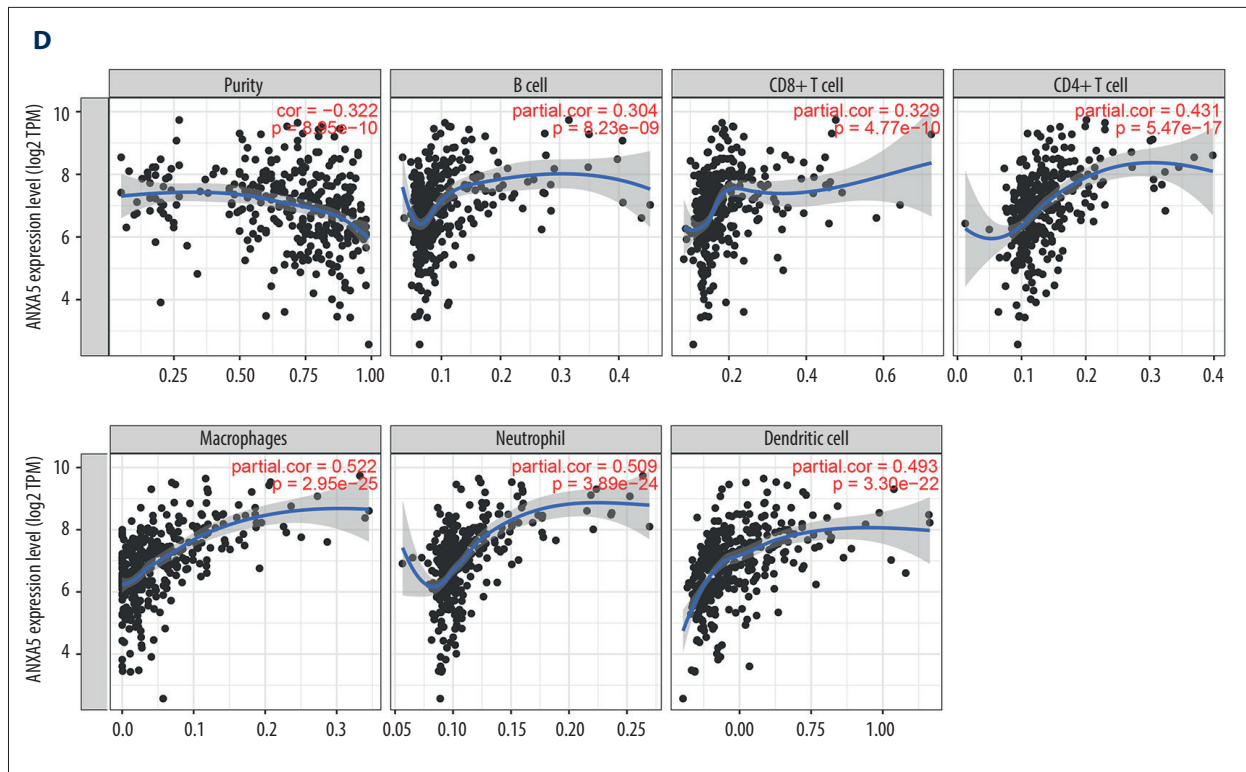


Figure 9. The relationship between ANXA5 and immune cell infiltration in hepatocellular carcinoma (HCC). (A, B) Survival curves of patient prognosis in monocytes and ANXA5 expression levels in HCC samples. (C) The relationship between mononuclear cell infiltration combined with ANXA5 expression level in HCC samples and patient prognosis. (D) Scatter plot of the correlation between ANXA5 and B cells, CD8 T cells, CD4 T cells, macrophages, neutrophils, and dendritic cells.

Currently, cancer research is advancing toward targeted therapies based on precision medicine guided by tumor mutations, thereby deepening our understanding of genomics, disease mechanisms, and drug development in the field [78]. For instance, combining genome sequencing with multi-omics molecular characterization analysis has accelerated the development of personalized interventions, such as CAR-T immunotherapy [79]. Our study comprehensively analyzed the potential roles of ARGs in HCC, particularly highlighting their significant impact on the tumor immune microenvironment. Importantly, we have identified promising candidates, like ANXA5, with ample evidence indicating its inseparable association with patient prognosis and immunity. These findings alleviate the challenges of clinical translation and provide crucial support for subsequent research endeavors.

To the best of our knowledge, this is the first study to investigate the combination of anoikis- and immune-related genes as a prognostic signature for HCC. However, our study has some limitations. First, the results need to be further validated with clinical samples and experimental data. Second, the biological function and mechanism of ANXA5 in HCC progression require further exploration. We plan to implant HCC cell lines with ANXA5 knockdown and normal HCC cell lines separately into mice to observe the potential effects of ANXA5

alteration on tumors in vivo. Third, while the analytical methods we used are reliable, the emergence of new analysis techniques with advancing technology can impose temporal limitations on data analysis.

Conclusions

In this study, we explored the correlation between ARGs and immune cell infiltration in HCC, leading to the development of a novel prognostic model based on 11 ARG-related lncRNAs. Notably, ANXA5, a key ARG, emerged as a significant player influencing patient prognosis and immune cell infiltration in HCC. Acknowledging the hypothesis-generating nature of our work, we believe these findings suggest a promising direction for further research, indicating the potential of ANXA5 as a novel target for HCC treatment.

Acknowledgments

We are highly thankful to our colleagues, who are not listed as an author of this manuscript, for their support in completing this study. We also acknowledge the role of institutes and departments involved in this study.

Declaration of Figures' Authenticity

All figures submitted have been created by the authors, who confirm that the images are original with no duplication and have not been previously published in whole or in part.

References:

1. Yang JD, Hainaut P, Gores GJ, et al. A global view of hepatocellular carcinoma: Trends, risk, prevention and management. *Nat Rev Gastroenterol Hepatol.* 2019;16(10):589-604
2. Hu C, Xin Z, Sun X, et al. Activation of ACLY by SEC63 deploys metabolic reprogramming to facilitate hepatocellular carcinoma metastasis upon endoplasmic reticulum stress. *J Exp Clin Cancer Res.* 2023;42(1):108
3. Mandlik DS, Mandlik SK, Choudhary HB. Immunotherapy for hepatocellular carcinoma: Current status and future perspectives. *World J Gastroenterol.* 2023;29(6):1054-75
4. Keren L, Bosse M, Marquez D, et al. A structured tumor-immune microenvironment in triple negative breast cancer revealed by multiplexed ion beam imaging. *Cell.* 2018;174(6):1373-87.e19
5. de Bono JS, Ashworth A. Translating cancer research into targeted therapeutics. *Nature.* 2010;467(7315):543-49
6. Oura K, Morishita A, Tani J, Masaki T. Tumor immune microenvironment and immunosuppressive therapy in hepatocellular carcinoma: A review. *Int J Mol Sci.* 2021;22(11):5801
7. Chen Y, Tian Z. HBV-induced immune imbalance in the development of HCC. *Front Immunol.* 2019;10:2048
8. Song G, Shi Y, Zhang M, et al. Global immune characterization of HBV/HCV-related hepatocellular carcinoma identifies macrophage and T-cell subsets associated with disease progression. *Cell Discov.* 2020;6(1):90
9. Sharma A, Seow JJW, Dutertre CA, et al. Onco-fetal reprogramming of endothelial cells drives immunosuppressive macrophages in hepatocellular carcinoma. *Cell.* 2020 Oct 15;183(2):377-94.e21
10. Cheng JT, Deng YN, Yi HM, et al. Hepatic carcinoma-associated fibroblasts induce IDO-producing regulatory dendritic cells through IL-6-mediated STAT3 activation. *Oncogenesis.* 2016;5(2):e198
11. Deng Y, Cheng J, Fu B, et al. Hepatic carcinoma-associated fibroblasts enhance immune suppression by facilitating the generation of myeloid-derived suppressor cells. *Oncogene.* 2017;36(8):1090-101
12. Bagaev A, Kotlov N, Nomie K, et al. Conserved pan-cancer microenvironment subtypes predict response to immunotherapy. *Cancer Cell.* 2021;39(6):845-865.e7
13. Adeshakin FO, Adeshakin AO, Afolabi LO, et al. Mechanisms for modulating anoikis resistance in cancer and the relevance of metabolic reprogramming. *Front Oncol.* 2021;11:626577
14. Guadamillas MC, Cerezo A, Del Pozo MA. Overcoming anoikis – pathways to anchorage-independent growth in cancer. *J Cell Sci.* 2011;124(Pt 19):3189-97
15. Shi T, Zhang C, Xia S. The potential roles and mechanisms of non-coding RNAs in cancer anoikis resistance. *Mol Cell Biochem.* 2022;477(5):1371-80
16. St Laurent G, Wahlestedt C, Kapranov P. The landscape of long non-coding RNA classification. *Trends Genet.* 2015;31(5):239-51
17. Robinson EK, Covarrubias S, Carpenter S. The how and why of lncRNA function: An innate immune perspective. *Biochim Biophys Acta Gene Regul Mech.* 2020;1863(4):194419
18. Bhan A, Soleimani M, Mandal SS. Long noncoding RNA and cancer: A new paradigm. *Cancer Res.* 2017;77(15):3965-81
19. Lv W, Wang Y, Zhao C, et al. Identification and validation of m6A-related lncRNA signature as potential predictive biomarkers in breast cancer. *Front Oncol.* 2021;11:745719
20. Lu Y, Luo X, Wang Q, et al. A novel necroptosis-related lncRNA signature predicts the prognosis of lung adenocarcinoma. *Front Genet.* 2022;13:862741
21. Deng Z, Li X, Shi Y, et al. A novel autophagy-related lncRNAs signature for prognostic prediction and clinical value in patients with pancreatic cancer. *Front Cell Dev Biol.* 2020;8:606817

Supplementary Table

Supplementary Table 1. The expression levels of 34 long non-coding RNAs (lncRNAs) and survival data.

Supplementary Table 2 available from the corresponding author on request.

22. Huang Z, Zhou JK, Peng Y, et al. The role of long noncoding RNAs in hepatocellular carcinoma. *Mol Cancer.* 2020;19(1):77
23. Xu K, Xia P, Gongye X, et al. A novel lncRNA RP11-386G11.10 reprograms lipid metabolism to promote hepatocellular carcinoma progression. *Mol Metab.* 2022;63:101540
24. Zhang B, Bao W, Zhang S, et al. lncRNA HEPFAL accelerates ferroptosis in hepatocellular carcinoma by regulating SLC7A11 ubiquitination. *Cell Death Dis.* 2022;13(8):734
25. Chen M, Zhang C, Liu W, et al. Long noncoding RNA LINC01234 promotes hepatocellular carcinoma progression through orchestrating aspartate metabolic reprogramming. *Mol Ther.* 2022;30(6):2354-69
26. Cancer Genome Atlas Research Network. Comprehensive and integrative genomic characterization of hepatocellular carcinoma. *Cell.* 2017;169(7):1327-41.e23
27. Ma L, Hernandez MO, Zhao Y, et al. Tumor cell biodiversity drives microenvironmental reprogramming in liver cancer. *Cancer Cell.* 2019;36(4):418-30.e6
28. Chen Y, Feng Y, Yan F, et al. A novel immune-related gene signature to identify the tumor microenvironment and prognose disease among patients with oral squamous cell carcinoma patients using ssGSEA: A bioinformatics and biological validation study. *Front Immunol.* 2022;13:922195
29. Hänzelmann S, Castelo R, Guinney J. GSVA: Gene set variation analysis for microarray and RNA-seq data. *BMC Bioinformatics.* 2013;14:7
30. Yin Y, Tian Y, Ren X, et al. Qualification of necroptosis-related lncRNA to forecast the treatment outcome, immune response, and therapeutic effect of kidney renal clear cell carcinoma. *J Oncol.* 2022;2022:3283343
31. Ritchie ME, Phipson B, Wu D, et al. limma powers differential expression analyses for RNA-sequencing and microarray studies. *Nucleic Acids Res.* 2015;43(7):e47
32. Zhang Y, He R, Lei X, et al. A novel pyroptosis-related signature for predicting prognosis and indicating immune microenvironment features in osteosarcoma. *Front Genet.* 2021;12:780780
33. Yoshihara K, Shahmoradgolli M, Martínez E, et al. Inferring tumour purity and stromal and immune cell admixture from expression data. *Nat Commun.* 2013;4:2612
34. Tibshirani R. The lasso method for variable selection in the Cox model. *Stat Med.* 1997;16(4):385-95
35. Simon N, Friedman J, Hastie T, Tibshirani R. Regularization paths for Cox's proportional hazards model via coordinate descent. *J Stat Softw.* 2011;39(5):1-13
36. Frost HR, Amos CI. Gene set selection via LASSO penalized regression (SLPR). *Nucleic Acids Res.* 2017;45(12):e114
37. Charoentong P, Finotello F, Angelova M, et al. Pan-cancer immunogenomic analyses reveal genotype-immunophenotype relationships and predictors of response to checkpoint blockade. *Cell Rep.* 2017;18(1):248-62
38. Newman AM, Liu CL, Green MR, et al. Robust enumeration of cell subsets from tissue expression profiles. *Nat Methods.* 2015;12(5):453-57
39. Chen B, Khodadoust MS, Liu CL, et al. Profiling tumor infiltrating immune cells with CIBERSORT. *Methods Mol Biol.* 2018;1711:243-59
40. Zhu K, Xiaoqi L, Deng W, Wang G, Fu B. Development and validation of a novel lipid metabolism-related gene prognostic signature and candidate drugs for patients with bladder cancer. *Lipids Health Dis.* 2021;20(1):146
41. Plattner C, Finotello F, Rieder D. Deconvoluting tumor-infiltrating immune cells from RNA-seq data using quanTIseq. *Methods Enzymol.* 2020;636:261-85
42. Aran D, Hu Z, Butte AJ. xCell: Digitally portraying the tissue cellular heterogeneity landscape. *Genome Biol.* 2017;18(1):220

43. Becht E, Giraldo NA, Lacroix L, et al. Estimating the population abundance of tissue-infiltrating immune and stromal cell populations using gene expression. *Genome Biol.* 2016;17(1):218 [Erratum in: *Genome Biol.* 2016;17(1):249]
44. Lu H, Wu J, Liang L, et al. Identifying a novel defined pyroptosis-associated long noncoding RNA signature contributes to predicting prognosis and tumor microenvironment of bladder cancer. *Front Immunol.* 2022;13:803355
45. Li T, Fan J, Wang B, et al. TIMER: A web server for comprehensive analysis of tumor-infiltrating immune cells. *Cancer Res.* 2017;77(21):e108-e10
46. Liu T, Yang K, Chen J, et al. Comprehensive pan-cancer analysis of KIF18A as a marker for prognosis and immunity. *Biomolecules.* 2023;13(2):326
47. Stuart T, Butler A, Hoffman P, et al. Comprehensive integration of single-cell data. *Cell.* 2019;177(7):1888-902.e21
48. Gribov A, Sill M, Lück S, et al. SEURAT: Visual analytics for the integrated analysis of microarray data. *BMC Med Genomics.* 2010;3:21
49. Korsunsky I, Millard N, Fan J, et al. Fast, sensitive and accurate integration of single-cell data with Harmony. *Nat Methods.* 2019;16(12):1289-96
50. Chen YC, Suresh A, Underbayev C, et al. IKAP-Identifying K mAjor cell population groups in single-cell RNA-sequencing analysis. *Gigascience.* 2019;8(10):giz121
51. Heumos L, Schaar AC, Lance C, et al; Single-cell Best Practices Consortium; Schiller HB, Theis FJ. Best practices for single-cell analysis across modalities. *Nat Rev Genet.* 2023;24(8):550-72
52. Aran D, Looney AP, Liu L, et al. Reference-based analysis of lung single-cell sequencing reveals a transitional profibrotic macrophage. *Nat Immunol.* 2019;20(2):163-72
53. Xu-Monette ZY, Zhang M, Li J, Young KH. PD-1/PD-L1 blockade: Have we found the key to unleash the antitumor immune response? *Front Immunol.* 2017;8:1597
54. Garon EB, Rizvi NA, Hui R, et al; KEYNOTE-001 Investigators. Pembrolizumab for the treatment of non-small-cell lung cancer. *N Engl J Med.* 2015;372(21):2018-28
55. Zhao Y, Zhang YN, Wang KT, Chen L. Lenvatinib for hepatocellular carcinoma: From preclinical mechanisms to anti-cancer therapy. *Biochim Biophys Acta Rev Cancer.* 2020;1874(1):188391
56. El-Khoueiry A. The promise of immunotherapy in the treatment of hepatocellular carcinoma. *Am Soc Clin Oncol Educ Book.* 2017;37:311-17
57. Wang Z, Zhu J, Liu Y, et al. Development and validation of a novel immune-related prognostic model in hepatocellular carcinoma. *J Transl Med.* 2020;18(1):67
58. Zhang C, Yang Y, Wang K, et al. The systematic analyses of RING finger gene signature for predicting the prognosis of patients with hepatocellular carcinoma. *J Oncol.* 2022;2022:2466006
59. Li B, Ren M, Zhou X, et al. Targeting tumor-associated macrophages in head and neck squamous cell carcinoma. *Oral Oncol.* 2020;106:104723
60. Zahran AM, Nafady-Hego H, Mansor SG, et al. Increased frequency and FOXP3 expression of human CD8+CD25High+ T lymphocytes and its relation to CD4 regulatory T cells in patients with hepatocellular carcinoma. *Hum Immunol.* 2019;80(7):510-16
61. Hassan EA, Ahmed EH, Nafee AM, et al. Regulatory T cells, IL10 and IL6 in HCV related hepatocellular carcinoma after transarterial chemoembolization (TACE). *Egypt J Immunol.* 2019;26(1):69-78
62. Zahran AM, Abdel-Meguid MM, Ashmawy AM, et al. Frequency and Implications of natural killer and natural killer T cells in hepatocellular carcinoma. *Egypt J Immunol.* 2018;25(2):45-52
63. Yahoo N, Dudek M, Knolle P, Heikenwälder M. Role of immune responses in the development of NAFLD-associated liver cancer and prospects for therapeutic modulation. *J Hepatol.* 2023;79(2):538-51
64. Shi F, Shi M, Zeng Z, et al. PD-1 and PD-L1 upregulation promotes CD8(+) T-cell apoptosis and postoperative recurrence in hepatocellular carcinoma patients. *Int J Cancer.* 2011;128(4):887-96
65. Ma C, Kesarwala AH, Eggert T, et al. NAFLD causes selective CD4(+) T lymphocyte loss and promotes hepatocarcinogenesis. *Nature.* 2016;531(7593):253-57
66. Zahran AM, Hetta HF, Rayan A, et al. Differential expression of Tim-3, PD-1, and CCR5 on peripheral T and B lymphocytes in hepatitis C virus-related hepatocellular carcinoma and their impact on treatment outcomes. *Cancer Immunol Immunother.* 2020;69(7):1253-63
67. Haber PK, Puigvehí M, Castet F, et al. Evidence-based management of hepatocellular carcinoma: Systematic review and meta-analysis of randomized controlled trials (2002-2020). *Gastroenterology.* 2021;161(3):879-98
68. Couri T, Pillai A. Goals and targets for personalized therapy for HCC. *Hepatol Int.* 2019;13(2):125-37
69. Ahluwalia P, Ahluwalia M, Mondal AK, et al. Immunogenomic gene signature of cell-death associated genes with prognostic implications in lung cancer. *Cancers (Basel).* 2021;13(1):155
70. Hu FF, Liu CJ, Liu LL, et al. Expression profile of immune checkpoint genes and their roles in predicting immunotherapy response. *Brief Bioinform.* 2021;22(3):bbaa176
71. Andree HA, Reutelingsperger CP, Hauptmann R, et al. Binding of vascular anticoagulant alpha (VAC alpha) to planar phospholipid bilayers. *J Biol Chem.* 1990;265(9):4923-28
72. Koopman G, Reutelingsperger CP, Kuijten GA, et al. Annexin V for flow cytometric detection of phosphatidylserine expression on B cells undergoing apoptosis. *Blood.* 1994;84(5):1415-20
73. Stach CM, Turnay X, Voll RE, et al. Treatment with annexin V increases immunogenicity of apoptotic human T-cells in Balb/c mice. *Cell Death Differ.* 2000;7(10):911-15
74. Frey B, Schildkopf P, Rödel F, et al. AnnexinA5 renders dead tumor cells immunogenic – implications for multimodal cancer therapies. *J Immunotoxicol.* 2009;6(4):209-16
75. Liu K, Liu J, Zhang X, et al. Identification of a Novel CD8+ T cell exhaustion-related gene signature for predicting survival in hepatocellular carcinoma. *BMC Cancer.* 2023;23(1):1185
76. Chaurio RA, Janko C, Muñoz LE, et al. Phospholipids: Key players in apoptosis and immune regulation. *Molecules.* 2009;14(12):4892-914
77. Kang TH, Park JH, Yang A, et al. Annexin A5 as an immune checkpoint inhibitor and tumor-homing molecule for cancer treatment. *Nat Commun.* 2020;11(1):1137
78. Zeggini E, Gloy AL, Barton AC, Wain LV. Translational genomics and precision medicine: Moving from the lab to the clinic. *Science.* 2019;365(6460):1409-13
79. Sterner RC, Sterner RM. CAR-T cell therapy: Current limitations and potential strategies. *Blood Cancer J.* 2021;11(4):69